UNCLASSIFIED

~~RESTRICTED~~

Copy No. 5

RM No. L8E07

NACA RM No. L8E07

CLASSIFICATION CHANGED 11 NOV 1948

To UNCLASSIFIED

NACA

By authority of H. L. Dryden Date Nov. 26, 1952
per NACA Release form #1346.
By HJR, 12-24-52

RESEARCH MEMORANDUM

AERODYNAMIC CHARACTERISTICS AT HIGH SPEEDS OF FULL-SCALE PROPELLERS HAVING CLARK Y BLADE SECTIONS

By

Peter J. Johnson

Langley Aeronautical Laboratory
Langley Field, Va.

CLASSIFIED DOCUMENT

This document contains classified information affecting the National Defense of the United States within the meaning of the Espionage Act, USC 50:31 and 32. Its transmission or the revelation of its contents in any manner to an unauthorized person is prohibited by law. Information so classified may be imparted only to persons in the military and naval services of the United States, appropriate civilian officers and employees of the Federal Government who have a legitimate interest therein, and to United States citizens of known loyalty and discretion who of necessity must be informed thereof.

NATIONAL ADVISORY COMMITTEE FOR AERONAUTICS

WASHINGTON
October 26, 1948

N A C A LIBRARY
LANGLEY MEMORIAL AERONAUTICAL LABORATORY
Langley Field, Va.

~~RESTRICTED~~

UNCLASSIFIED

NASA Technical Library
3 1176 01436 6547

NATIONAL ADVISORY COMMITTEE FOR AERONAUTICS

RESEARCH MEMORANDUM

AERODYNAMIC CHARACTERISTICS AT HIGH SPEEDS OF FULL-SCALE PROPELLERS HAVING CLARK Y BLADE SECTIONS

By Peter J. Johnson

SUMMARY

Tests of two 10-foot-diameter, two-blade propellers having Clark Y blade sections have been made in the Langley 16-foot high-speed tunnel. The propellers, designated as NACA 10-(4)(08)-03CY and NACA 10-(4)(08)-03RCY, were tested on a 2000-horsepower dynamometer through a range of blade angles from 20° to 55° and at airspeeds varying from 60 to 485 miles per hour. The NACA 10-(4)(08)-03CY propeller had efficient airfoil sections extending to the spinner surface, and the NACA 10-(4)(08)-03RCY propeller represents a structural compromise having cylindrical shanks typical of conventional propellers.

The results of these tests are presented with no attempt having been made to analyze or compare the data with other high-speed-propeller test results. Envelope efficiencies of over 0.90 are attained for both propellers at the lower rotational speeds where the adverse effects of compressibility are small. At the higher rotational speeds the envelope efficiencies of both propellers are much lower. For the design blade angle of 45° the maximum efficiency of the NACA 10-(4)(08)-03CY propeller drops from 0.92 to 0.745 for an increase in helical-tip Mach numbers from 0.85 to 1.08. The corresponding loss in maximum efficiency for the NACA 10-(4)(08)-03RCY propeller is from 0.90 to 0.665.

INTRODUCTION

A general investigation is being made in the Langley 16-foot high-speed tunnel to determine the combined influence of propeller design parameters and air compressibility upon propeller performance. The propellers used are 10 feet in diameter, and the blade designs embody variations in blade width, thickness ratio, shank form, blade section, and design lift coefficient or camber. All of the blades were designed to operate with a minimum induced-energy loss when the blade angle of the 0.7 radius is 45° and the blade is operating at the design value of lift coefficient.

UNCLASSIFIED
~~RESTRICTED~~

The compressibility problem is very important in propeller design because blade-section speeds are higher than the speed of the airplane, and structural requirements lead to thick sections near the root. The solution of this problem led to the development of the 16-series airfoil sections which have high critical Mach numbers. Most of the blades in the series of NACA designs have the 16-series blade sections, but two of the blade designs have the older Clark Y blade sections so that a comparison can be made at high speeds with the blades having the newer 16-series sections.

The single purpose of this paper is to make available the data obtained from tests of these two Clark Y section propellers as quickly as possible with no attempt being made to analyze the results or to compare them with other high-speed-propeller test results.

SYMBOLS

b	blade width of chord, feet or inches
C_P	power coefficient $\left(P/\rho n^3 D^5\right)$
C_T	thrust coefficient $\left(T/\rho n^2 D^4\right)$
c_{l_d}	design section lift coefficient
D	propeller diameter, feet
h	blade section maximum thickness
J	advance ratio (V/nD)
M	Mach number of advance
M_t	helical-tip Mach number $\left(M\sqrt{1 + \left(\frac{\pi}{J}\right)^2}\right)$
n	propeller rotational speed, rps
P	power, foot-pounds per second
R	propeller tip radius, feet
r	radius to blade element, feet
T	thrust, pounds
V	velocity of advance, feet per second

β blade angle, degrees

$\beta_{0.75R}$ blade angle at 0.75 radius station

η propeller efficiency $\left(\frac{C_T}{C_P} J\right)$

ρ mass density of air, slugs per cubic foot

APPARATUS

A 2000-horsepower dynamometer (fig. 1) was used to test the propellers in the Langley 16-foot high-speed tunnel. The dynamometer, control equipment, instrumentation, and calibration are described in detail in reference 1.

Propeller blades.- Basic test data are presented graphically herein for the two-blade NACA 10-(4)(08)-03CY and NACA 10-(4)(08)-03RCY propellers. The significance of the digits and letters in the propeller designations are as follows: the digits in the first group give the propeller diameter; the digit in the first parenthesis is ten times the basic design lift coefficient at the 0.7 radius; the digits in the second parenthesis give the thickness ratio at the 0.7 radius; the digits in the third group give the solidity per blade at the 0.7 radius; the letter R indicates a blade with conventional round shank; and the letters CY identify the blade sections as Clark Y.

The blade-form curves for the NACA 10-(4)(08)-03CY and NACA 10-(4)(08)-03RCY blades are shown in figure 2. The NACA 10-(4)(08)-03CY propeller has efficient sections from the tip to the 0.2 radius, whereas the NACA 10-(4)(08)-03RCY propeller represents a structural compromise having the cylindrical shanks typical of some conventional propellers. For this propeller a minimum induced-energy loss is maintained except for the rounded sections near the spinner surface. Figures 3 and 4 are photographs of the blades, and figure 5 shows a comparison of the shank sections at two radii.

TESTS AND REDUCTION OF DATA

The range of blade angles and rotational speeds for the propellers tested is presented in table I. Thrust, torque, and rotational speed were measured for each of the blade angles in the table for various values of advance ratio as described in reference 1. For the constant rotational speeds, the advance ratio was varied by regulating the tunnel airspeed. The higher blade-angle tests were run only at the lower rotational speeds because the dynamometer could not deliver sufficient torque to cover the

complete range of advance ratio. The tests in which the rotational speed was varied were made to obtain data at high helical-tip Mach numbers with the propeller operating at the design blade angle of 45°.

The test data corrected for tunnel-wall interference and spinner forces (reference 1) are presented in the form of the usual thrust and power coefficients and propeller efficiency. Propeller thrust, as used in this paper, is defined as the shaft tension caused by the portion of the blades rotating in the air stream. The reduction of the test data is outlined in detail in reference 1.

Several of the test runs were repeated during and at the end of the test program. The results of these tests agreed closely with the original, indicating the total error in the basic data to be less than 1 percent for comparisons of data obtained in this sequence of tests.

RESULTS

The faired curves of thrust coefficient, power coefficient, and propeller efficiency plotted against advance ratio for the tests of NACA 10-(4)(08)-03CY and NACA 10-(4)(08)-03RCY propellers are presented in figures 6 through 19. The test points are shown on the graphs of thrust and power coefficients. The variation of helical-tip Mach number and air-stream Mach number with advance ratio appears on the figures showing propeller efficiency.

The variation of propeller envelope efficiency with advance ratio for the various rotational speeds is presented in figure 20 for the NACA 10-(4)(08)-03CY propeller and in figure 21 for the NACA 10-(4)(08)-03RCY. Envelope efficiencies of over 0.90 were attained for both propellers at the lower rotational speeds where the adverse effects of compressibility are small. The range of advance ratio for which efficiencies of over 0.90 were attained is much smaller for the round-shank propeller than for the wide-shank propeller. The maximum efficiency for the wide-shank propeller is 0.93 and for the round-shank propeller is about 0.91. These maximum efficiencies occur at an advance ratio near 2.1 for which the propellers were designed. At the higher rotational speeds the envelope efficiencies of both propellers are much lower, and at 2160 rpm the maximum efficiency of the round-shank propeller is less than 0.80.

In figure 22 the envelope efficiency of the NACA 10-(4)(08)-03CY propeller at 1350 rpm is compared with the optimum efficiency of a two-blade propeller with the Betz minimum induced-energy loss loading. This optimum efficiency was calculated by a method (reference 2) neglecting all profile-drag losses for a two-blade propeller operating at the same values of power coefficient as were obtained with the NACA 10-(4)(08)-03CY propeller. The optimum efficiency takes into

account the induced losses, both axial and rotational. The difference between the envelope and optimum efficiency curves is attributed to profile-drag losses. This difference is approximately 2 percent at the point of maximum envelope efficiency. The corresponding curves for the round-shank propeller are shown in figure 23.

Figure 24 shows the effect of compressibility on the maximum efficiency of both Clark Y section propellers operating at the design blade angle of 45°. The maximum efficiencies of both propellers are plotted against helical-tip Mach number. The variation of air-stream Mach number with helical-tip Mach number is shown on the same figure. The maximum efficiency of the round-shank propeller is less than the efficiency of the wide-shank propeller throughout the range of Mach numbers, and the difference increases with increasing Mach number. From a helical-tip Mach number of 0.85 to 1.08 the maximum efficiency of the NACA 10-(4)(08)-03CY propeller drops from 0.92 to 0.745. The corresponding loss in maximum efficiency for the NACA 10-(4)(08)-03RCY propeller is from 0.90 to 0.665.

Langley Aeronautical Laboratory
National Advisory Committee for Aeronautics
Langley Field, Va.

REFERENCES

1. Corson, Blake W., Jr., and Maynard, Julian D.: The NACA 2000-Horsepower Propeller Dynamometer and Tests at High Speed of an NACA 10-(3)(08)-03 Two-Blade Propeller. NACA RM No. L7L29, 1948.

2. Crigler, John L., and Talkin, Herbert W.: Charts for Determining Propeller Efficiency. NACA ACR No. L4I29, 1944.

TABLE I

ROTATIONAL SPEEDS AND BLADE-ANGLE SETTINGS FOR TESTS OF

NACA 10-(4)(08)-03CY AND 10-(4)(08)-03RCY PROPELLERS

Figure	Rotational speed (rpm)	$\beta_{0.75R}$ (deg)							
NACA 10-(4)(08)-03CY two-blade propeller									
6	1140			30	35	40	45	50	55
7	1350	20	25	30	35	40	45	50	
8	1500						45		
9	1600	20	25	30	35	40	45		
10	2000	20	25	30	35				
11	2160	20	25	30					
12	Varied						45		
NACA 10-(4)(08)-03RCY two-blade propeller									
13	1140				35	40	45	50	55
14	1350	20	25	30	35	40	45	50	
15	1500						45		
16	1600	20	25	30	35	40	45		
17	2000	20	25	30	35				
18	2160	20	25	30					
19	Varied						45		

NACA

Figure 1.- Propeller mounted on dynamometer in test section with tunnel open.

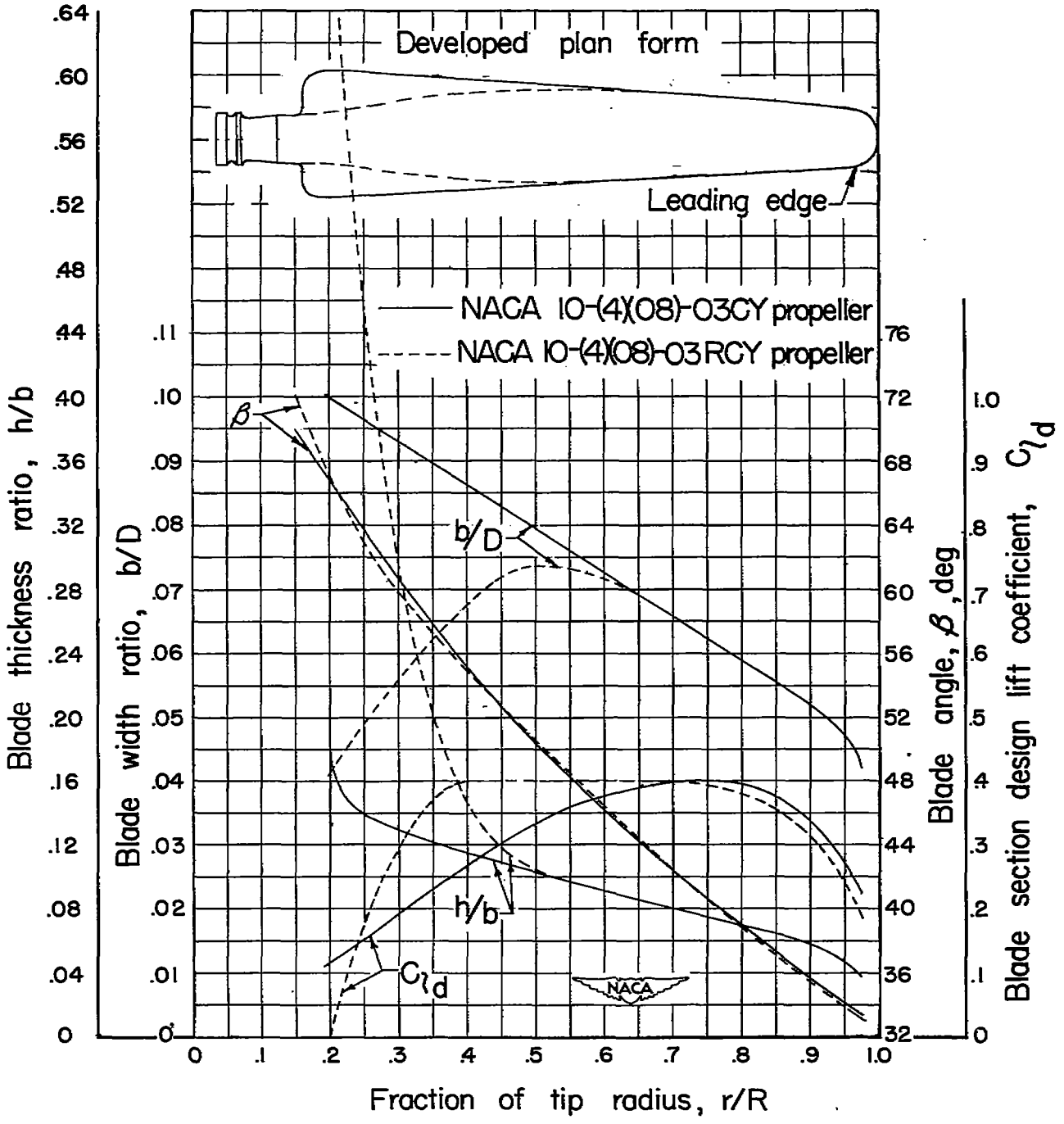

Figure 2.- Blade-form curves for NACA 10-(4)(08)-03CY and 10-(4)(08)-03RCY propellers.

Figure 3.- Photograph showing plan form of NACA 10-(4)(08)-0 propeller blades.

L-46148

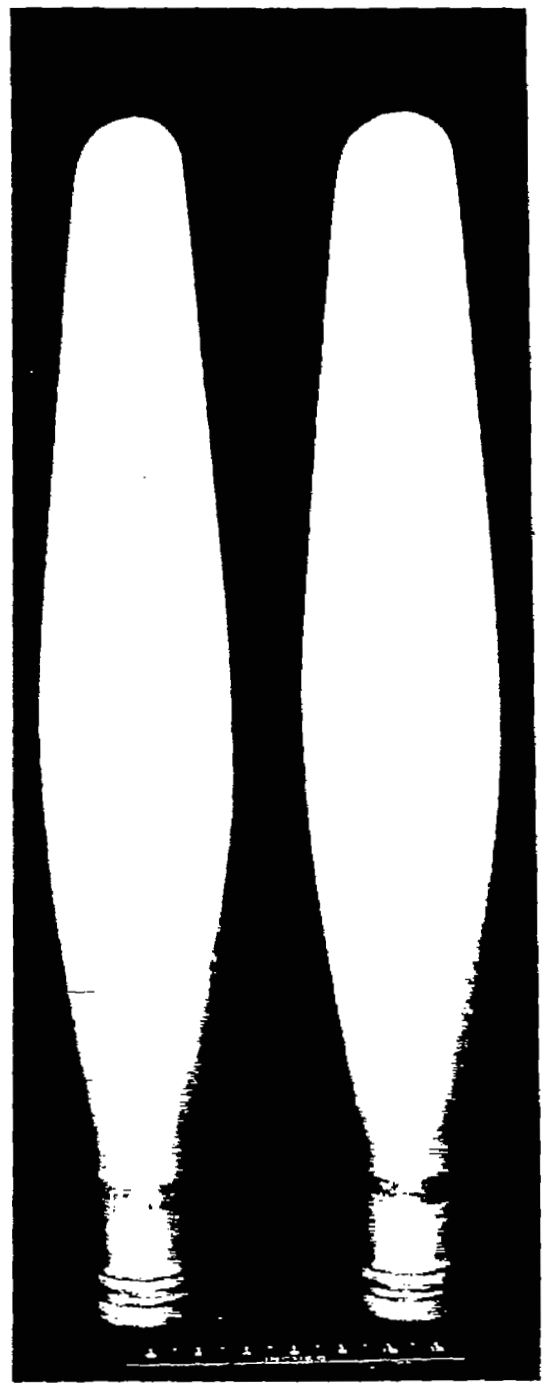

Figure 4.- Photograph showing plan form of NACA 10-(4)(08)-03RCY propeller blades.

L-46147

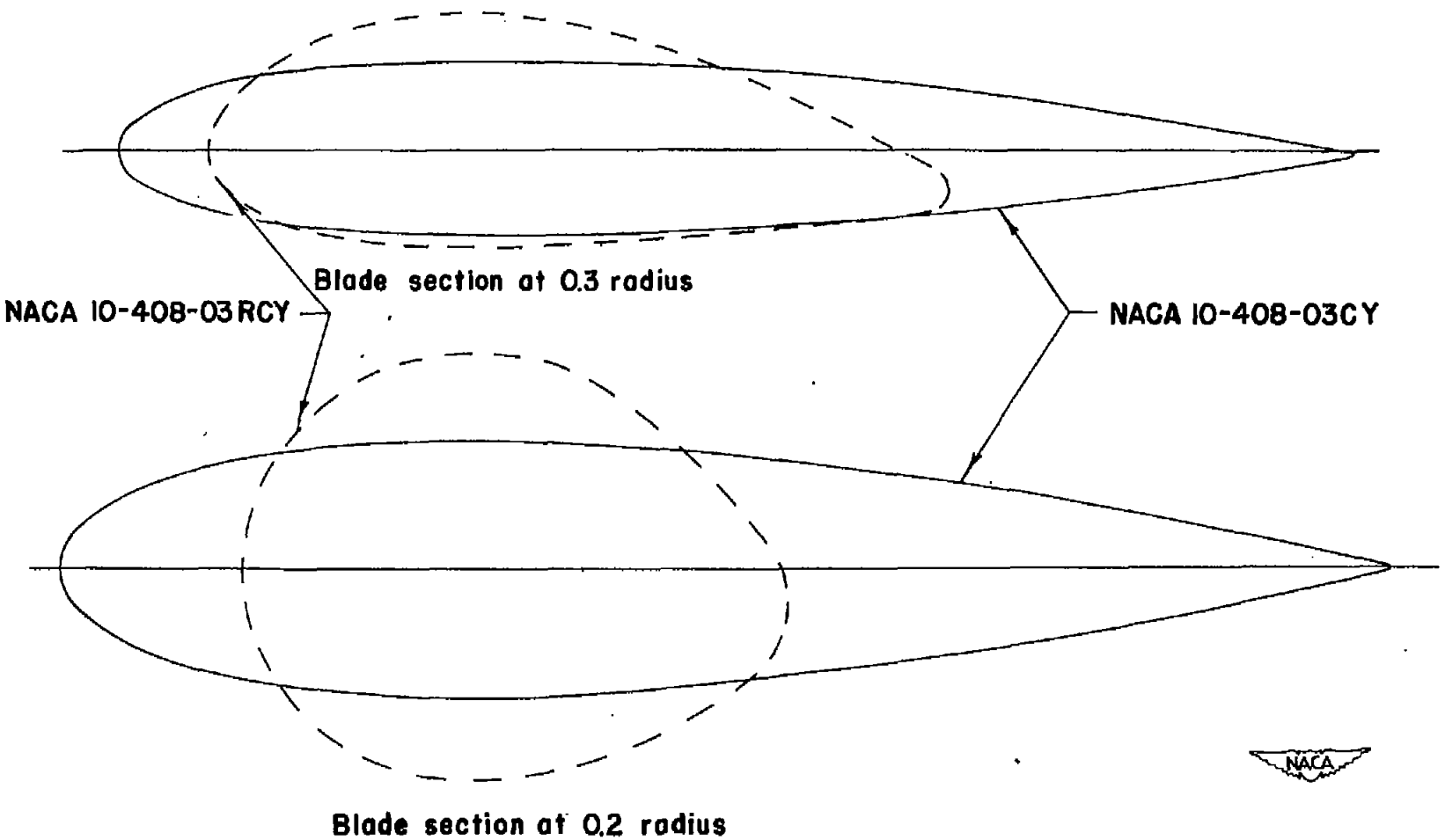

Figure 5.- Shank sections of NACA 10-(4)(08)-03CY and 10-(4)(08)-03RCY propeller blades.

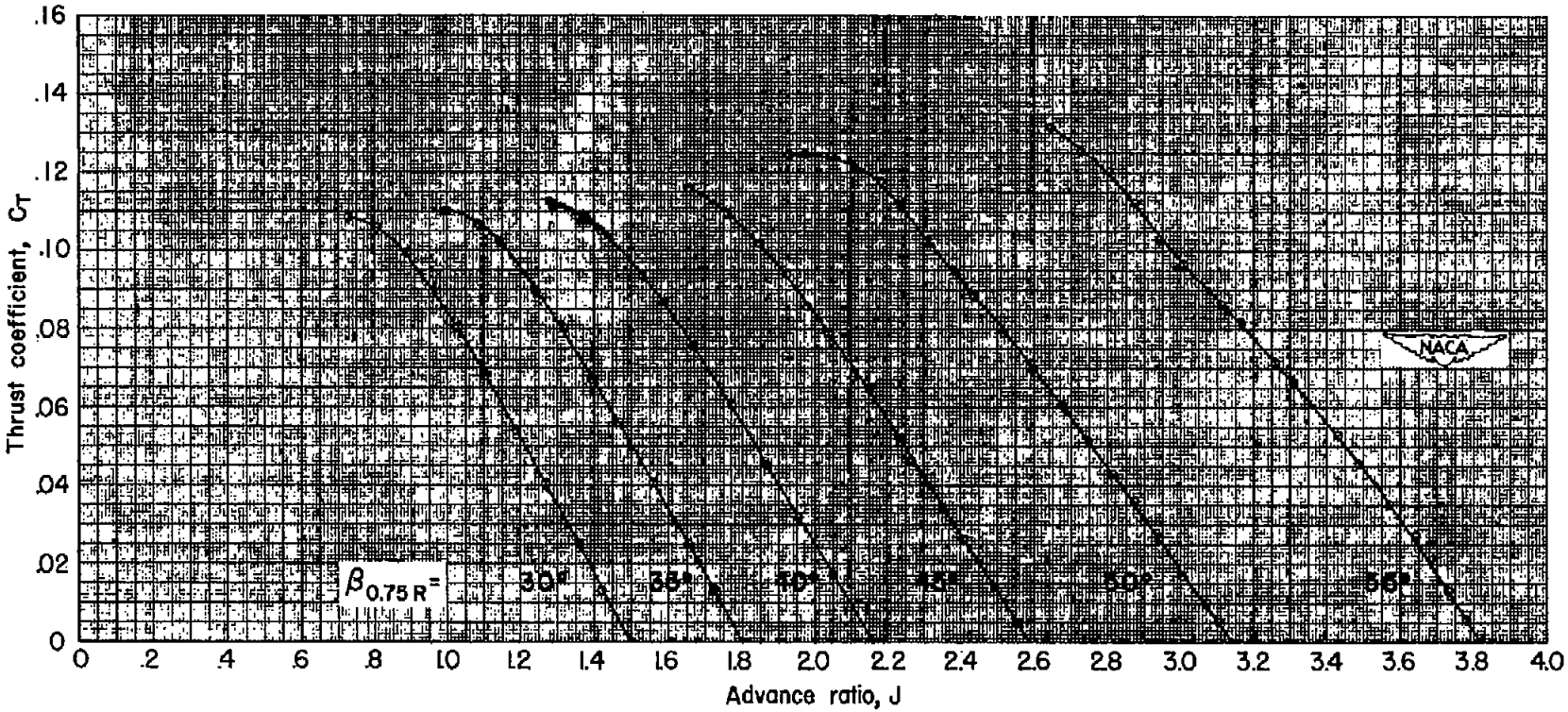

(a) Thrust coefficient.

Figure 6.- Characteristics of NACA 10-(4)(08)-03CY propeller. Rotational speed, 1140 rpm.

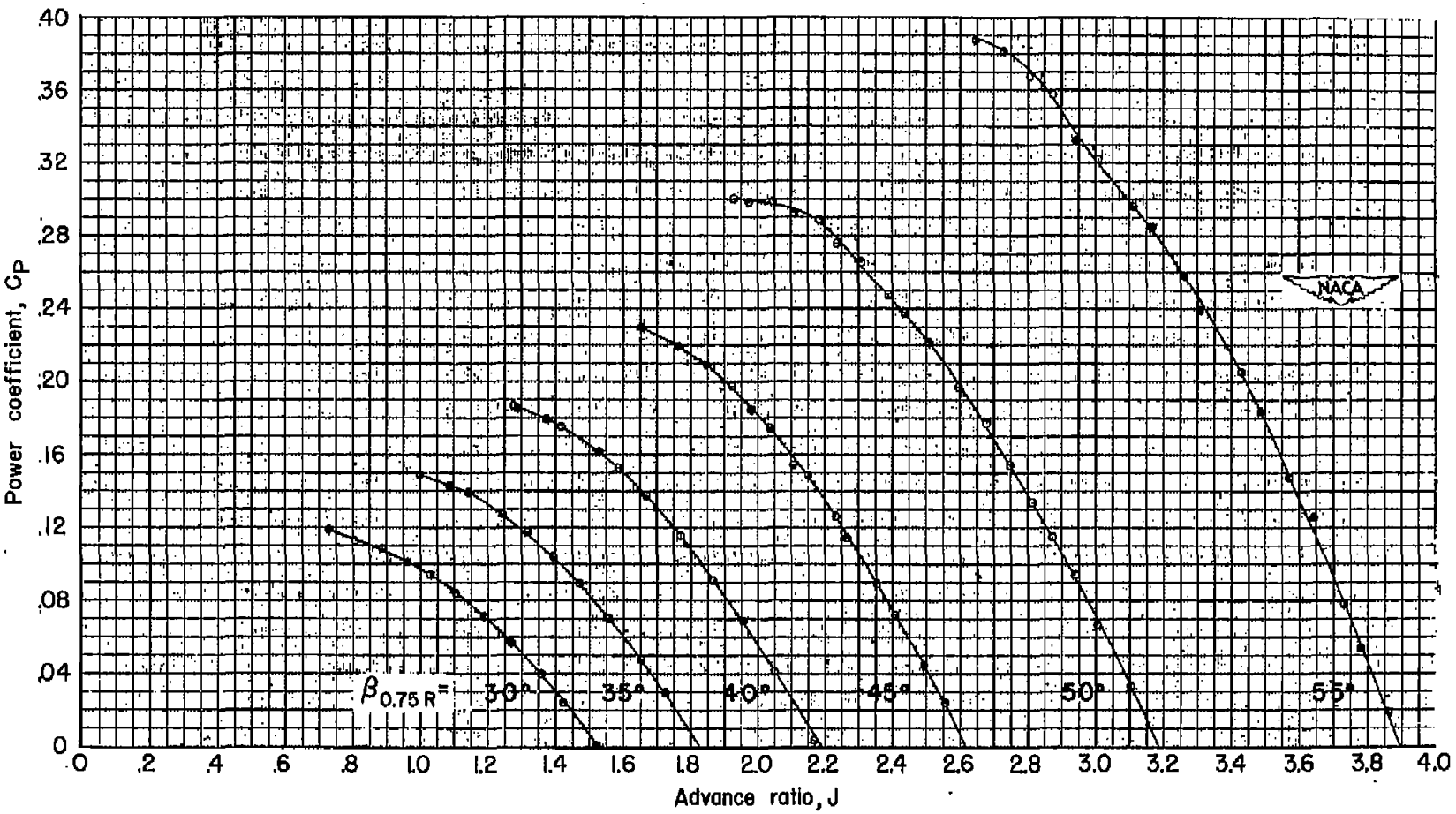

(b) Power coefficient.

Figure 6.- Continued. Rotational speed, 1140 rpm.

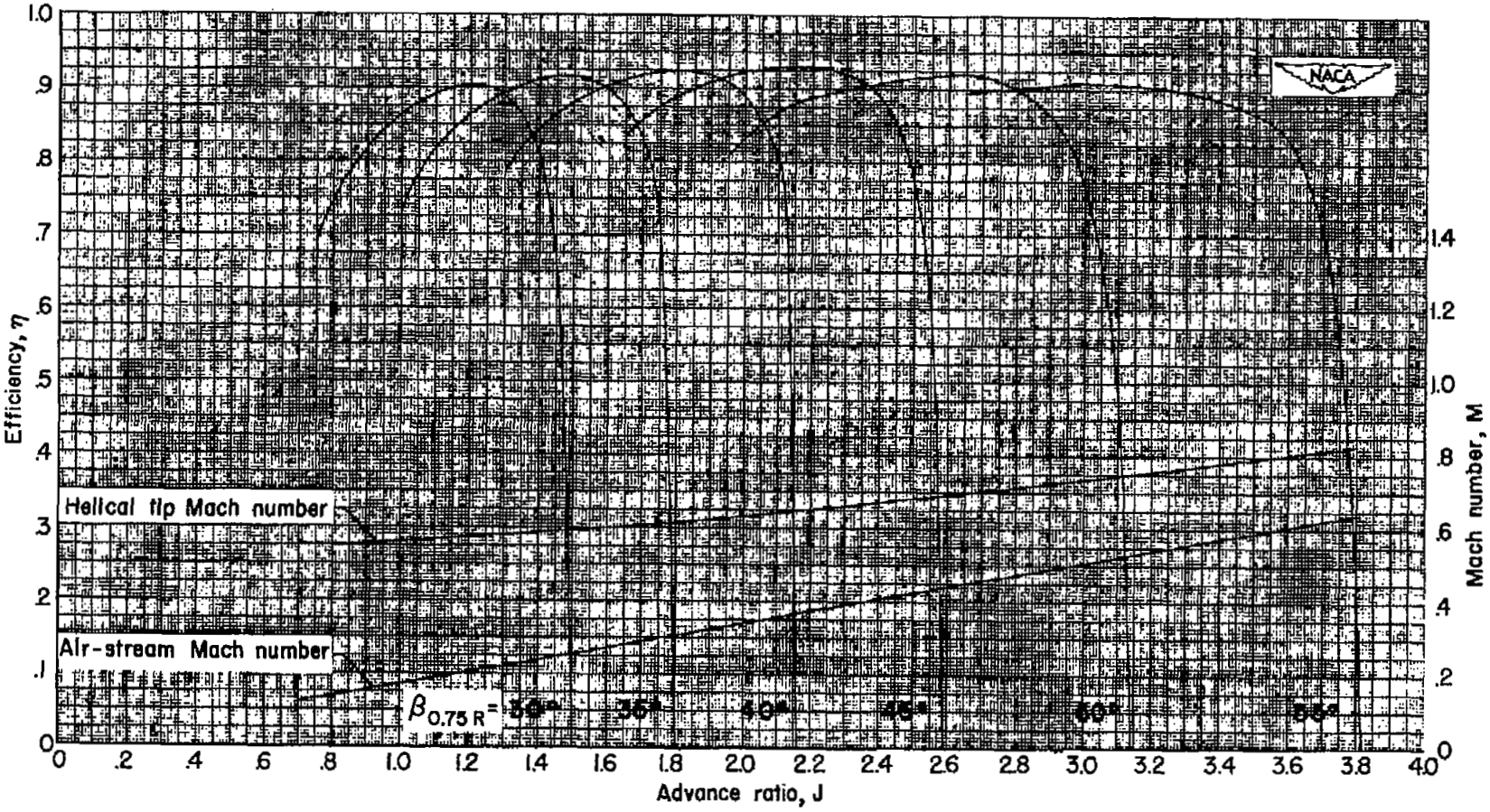

(c) Efficiency.

Figure 6:- Concluded. Rotational speed, 1140 rpm.

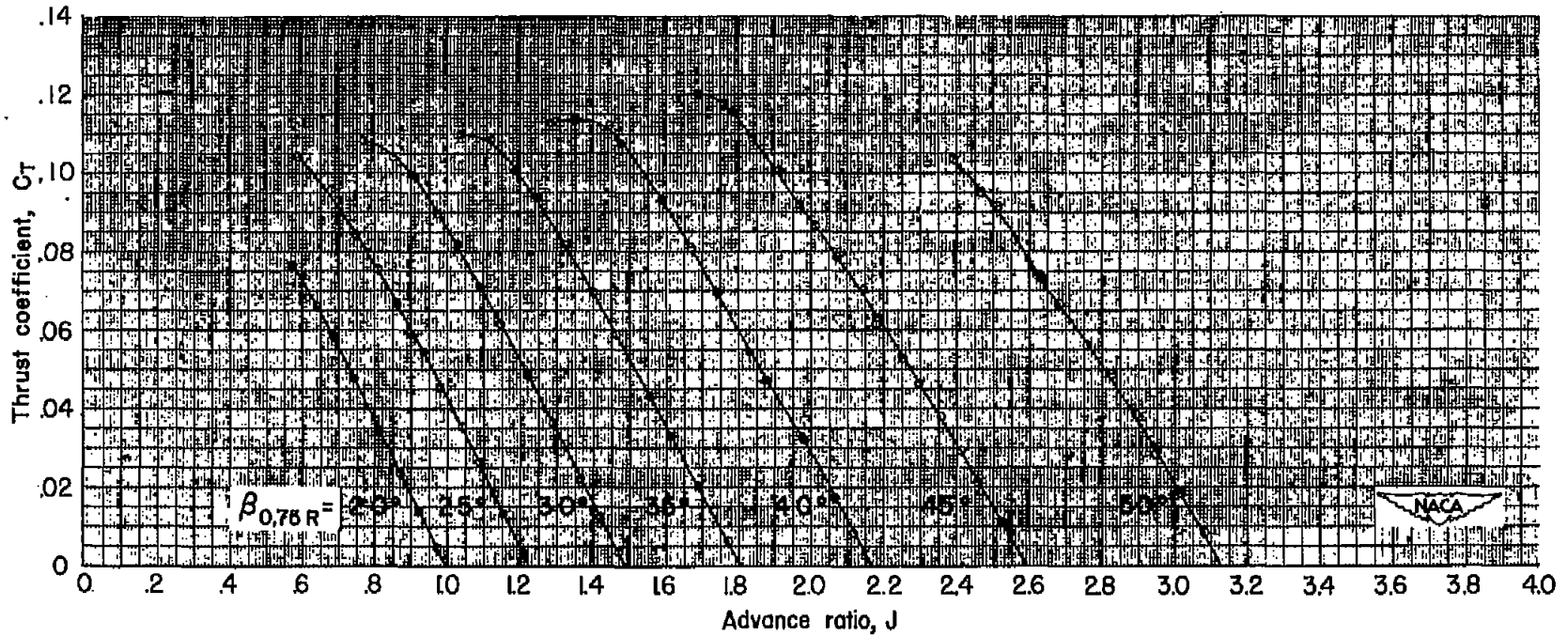

(a) Thrust coefficient.

Figure 7.- Characteristics of NACA 10-(4)(08)-03CY propeller. Rotational speed, 1350 rpm.

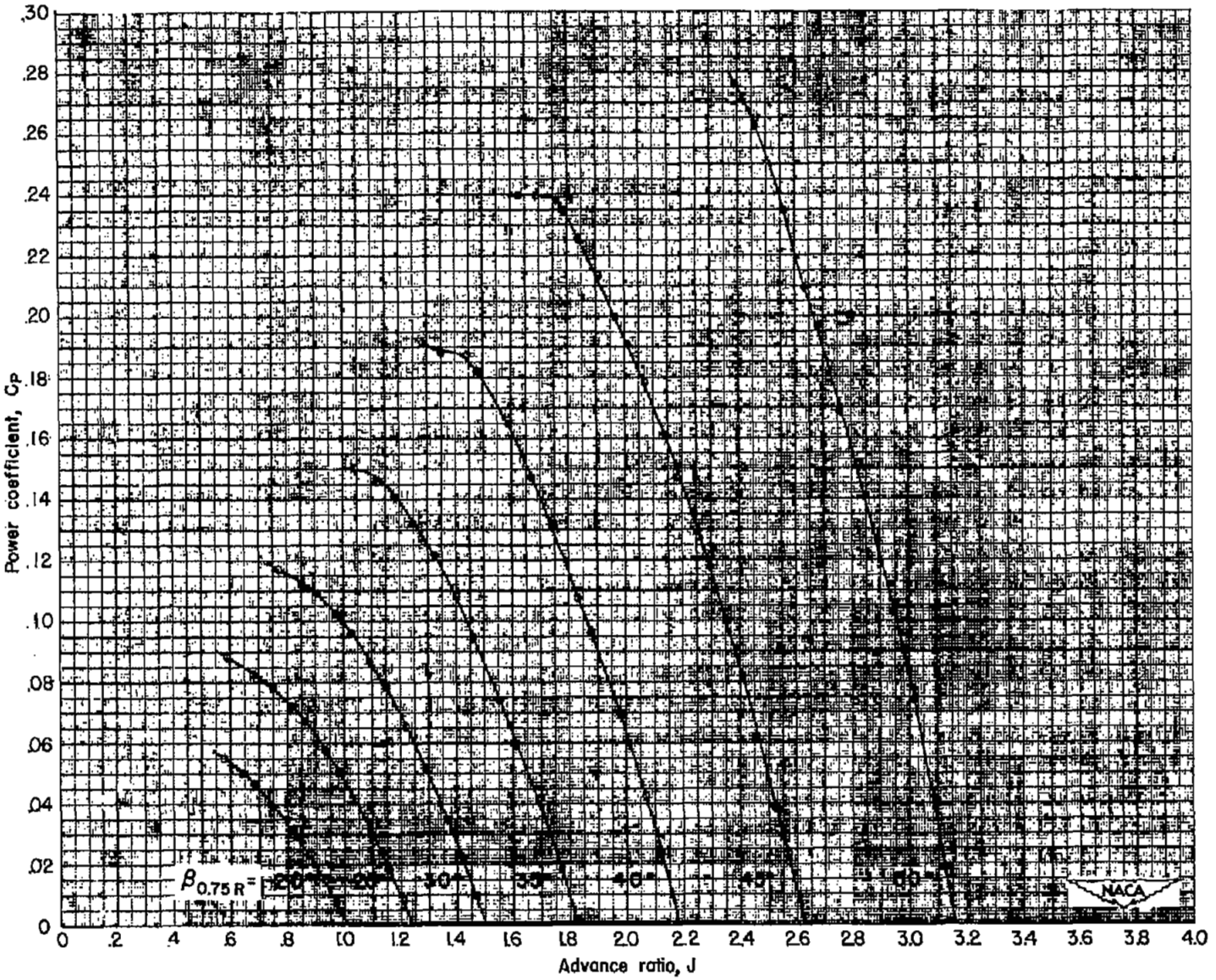

(b) Power coefficient.

Figure 7.- Continued. Rotational speed, 1350 rpm.

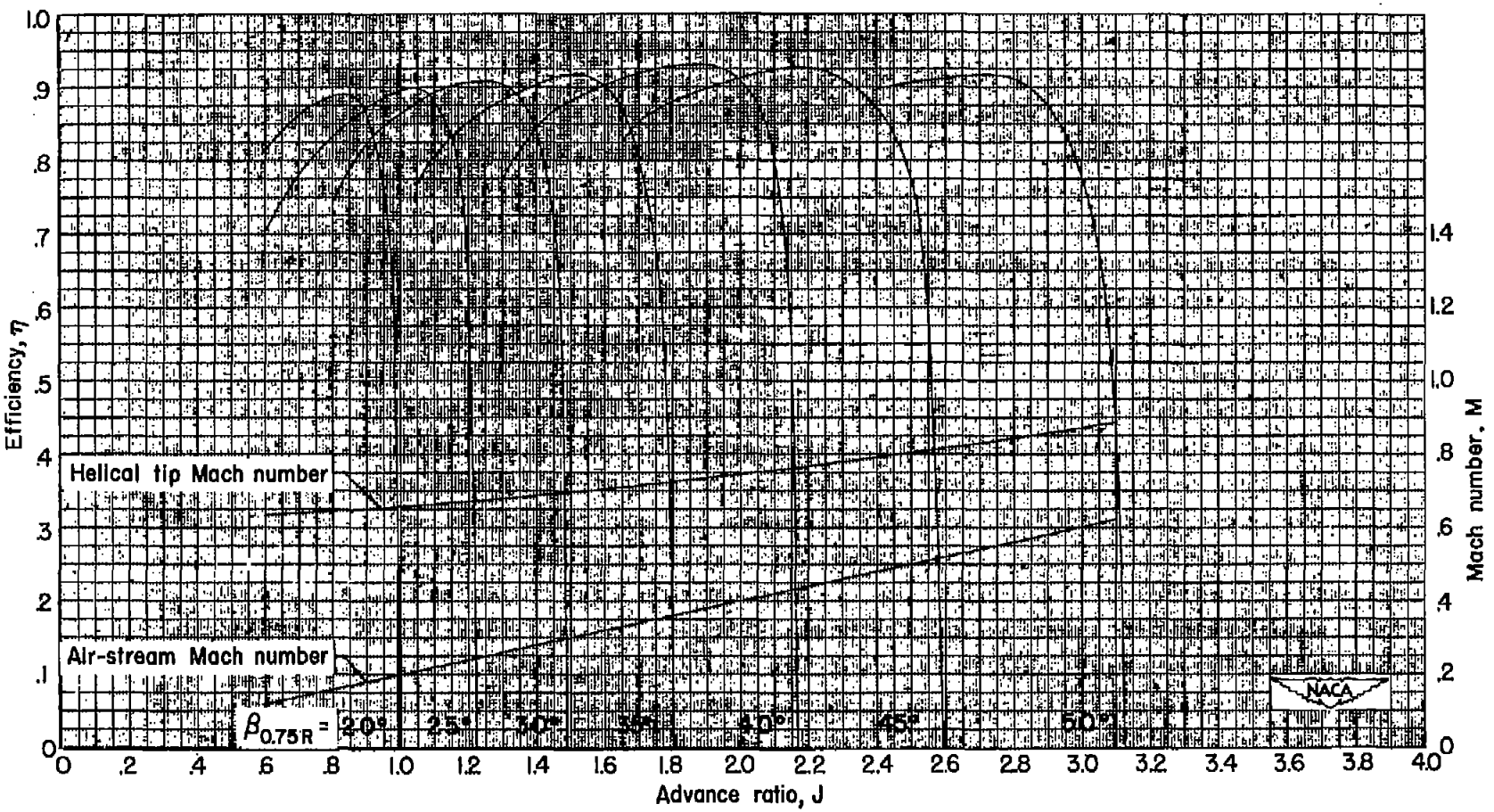

(c) Efficiency.

Figure 7.- Concluded. Rotational speed, 1350 rpm.

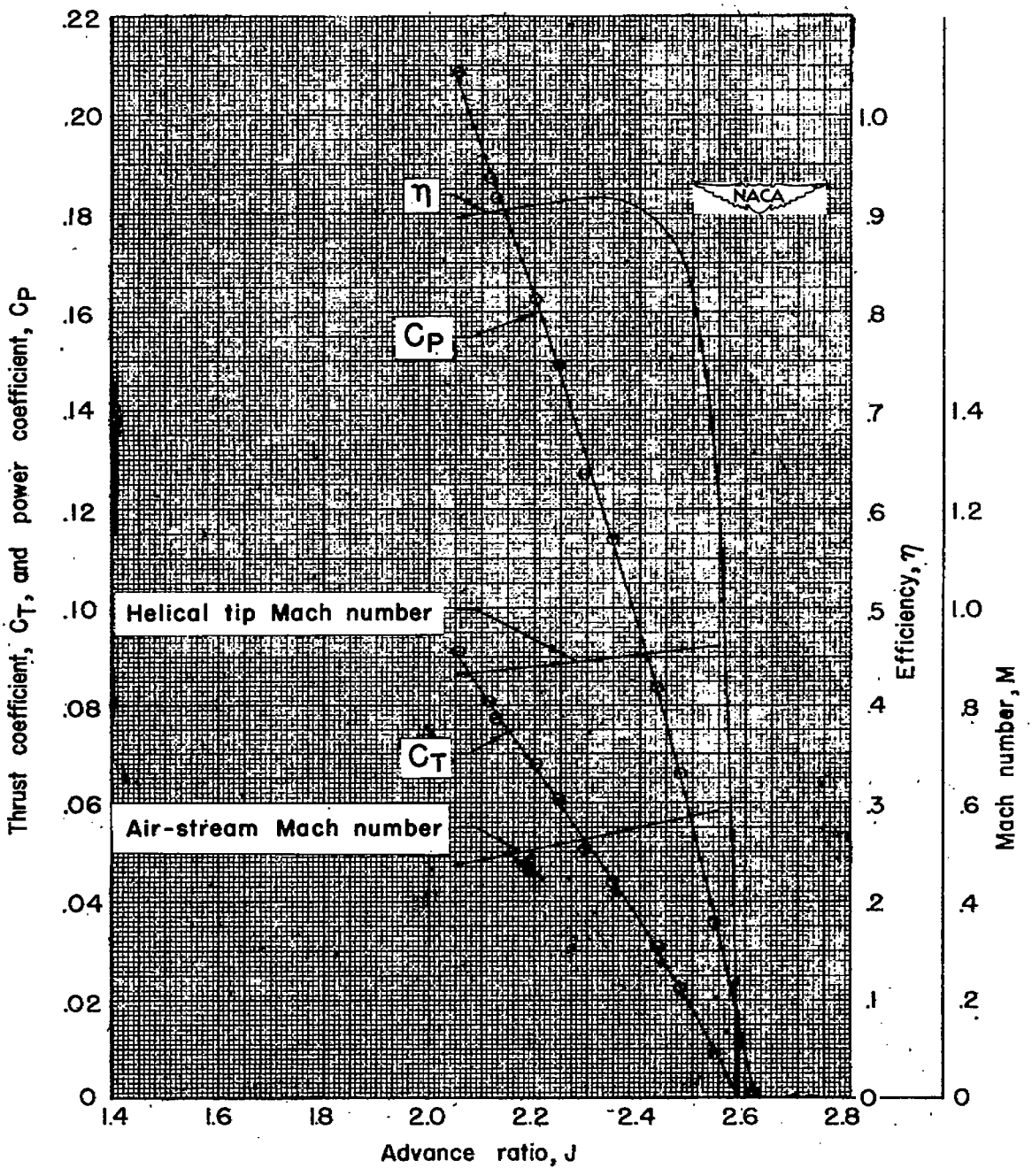

Figure 8.- Characteristics of NACA 10-(4)(08)-03CY propeller. Rotational speed, 1500 rpm. $\beta_{0.75R} = 45^{\circ}$.

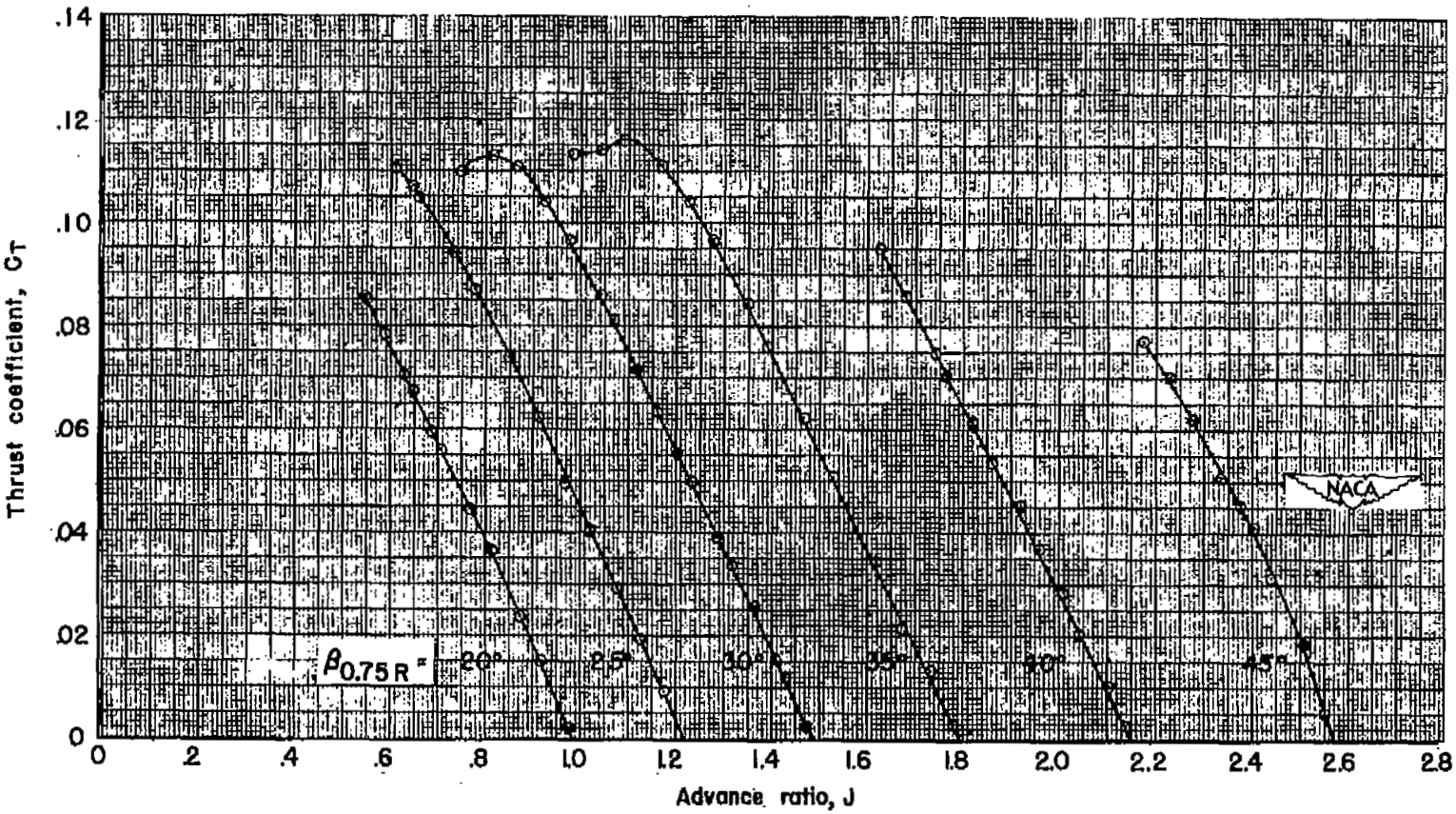

(a) Thrust coefficient.

Figure 9.- Characteristics of NACA 10-(4)(08)-03CY propeller. Rotational speed, 1600 rpm.

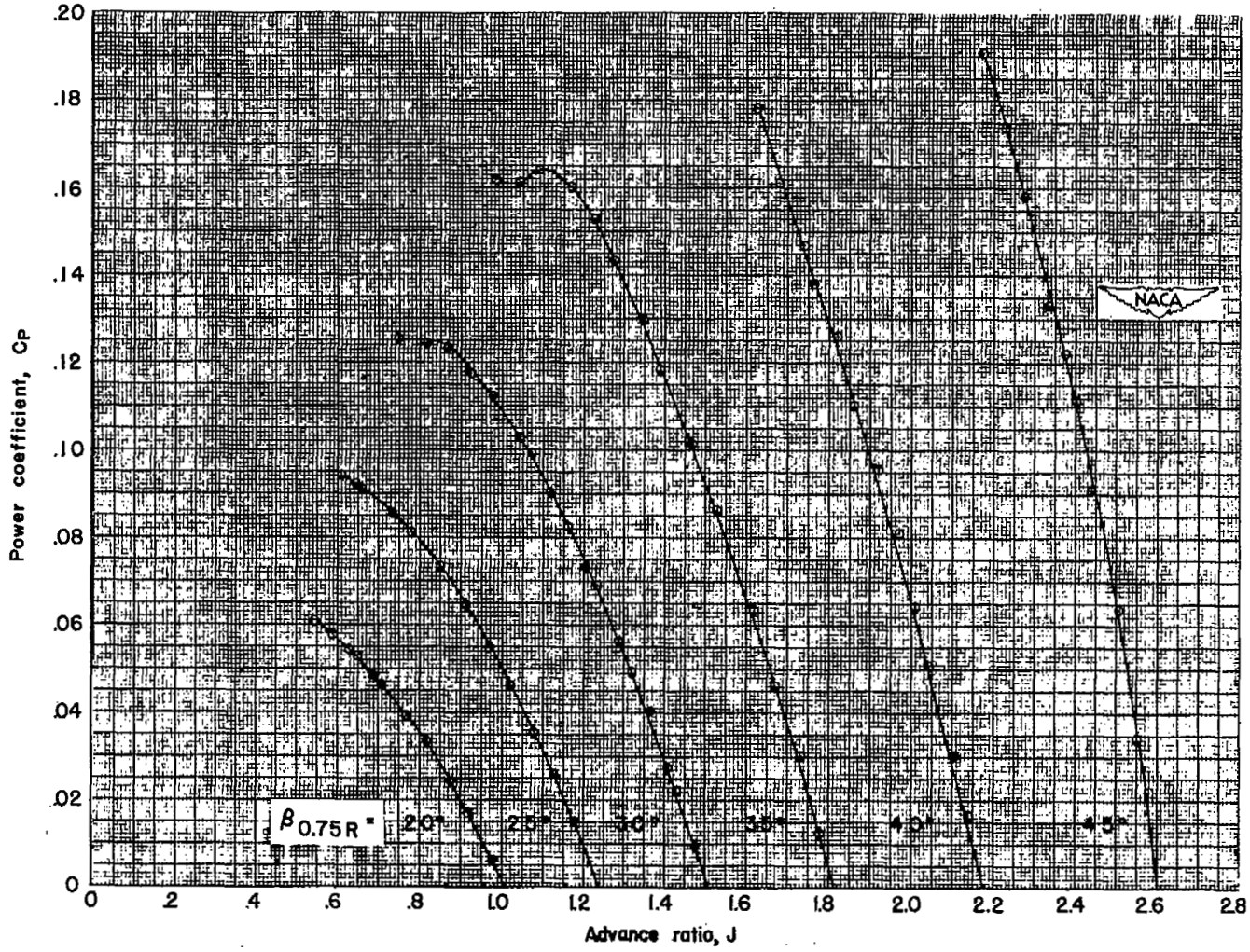

(b) Power coefficient.

Figure 9.- Continued. Rotational speed, 1600 rpm.

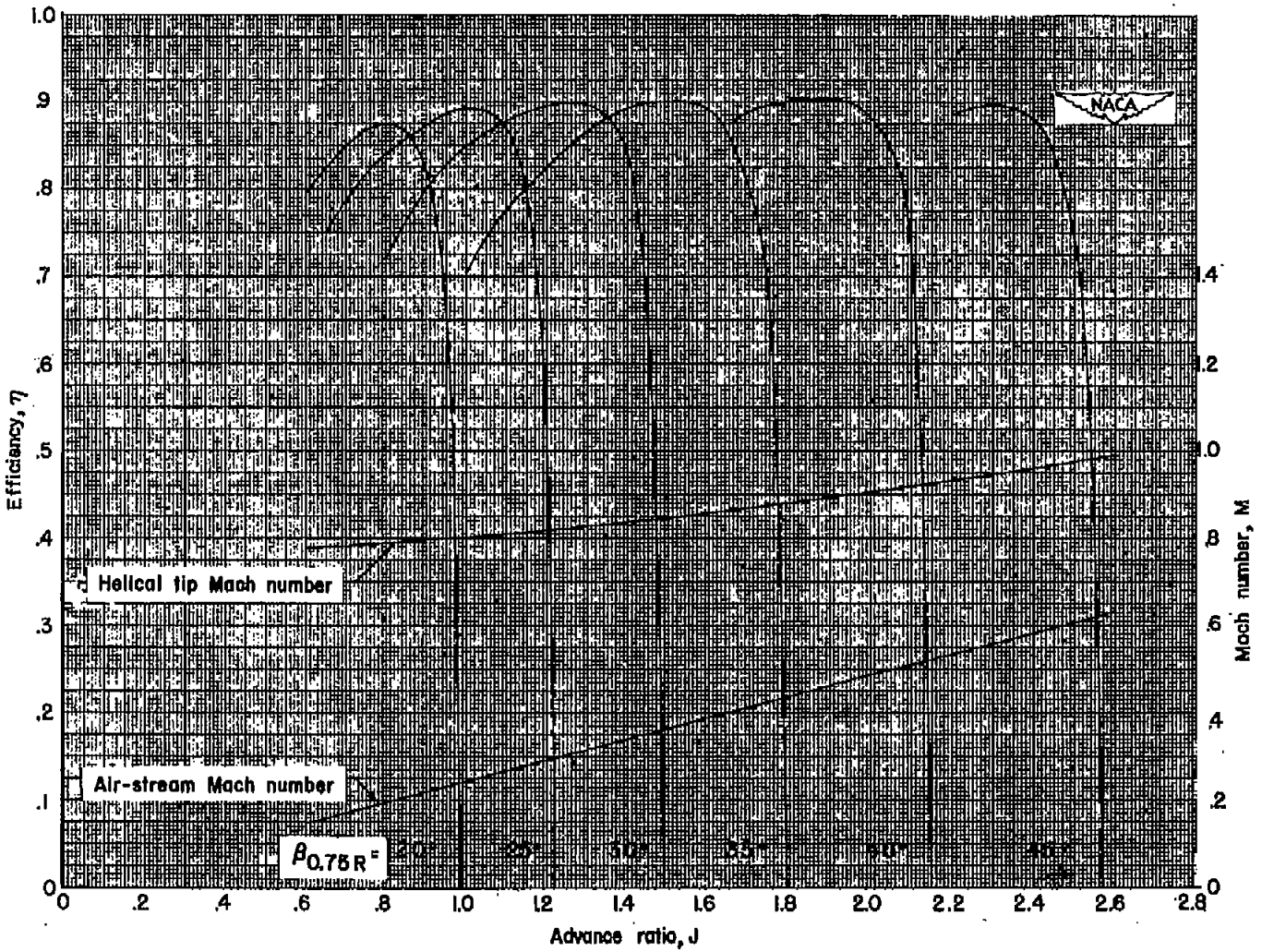

(c) Efficiency.

Figure 9.- Concluded. Rotational speed, 1600 rpm.

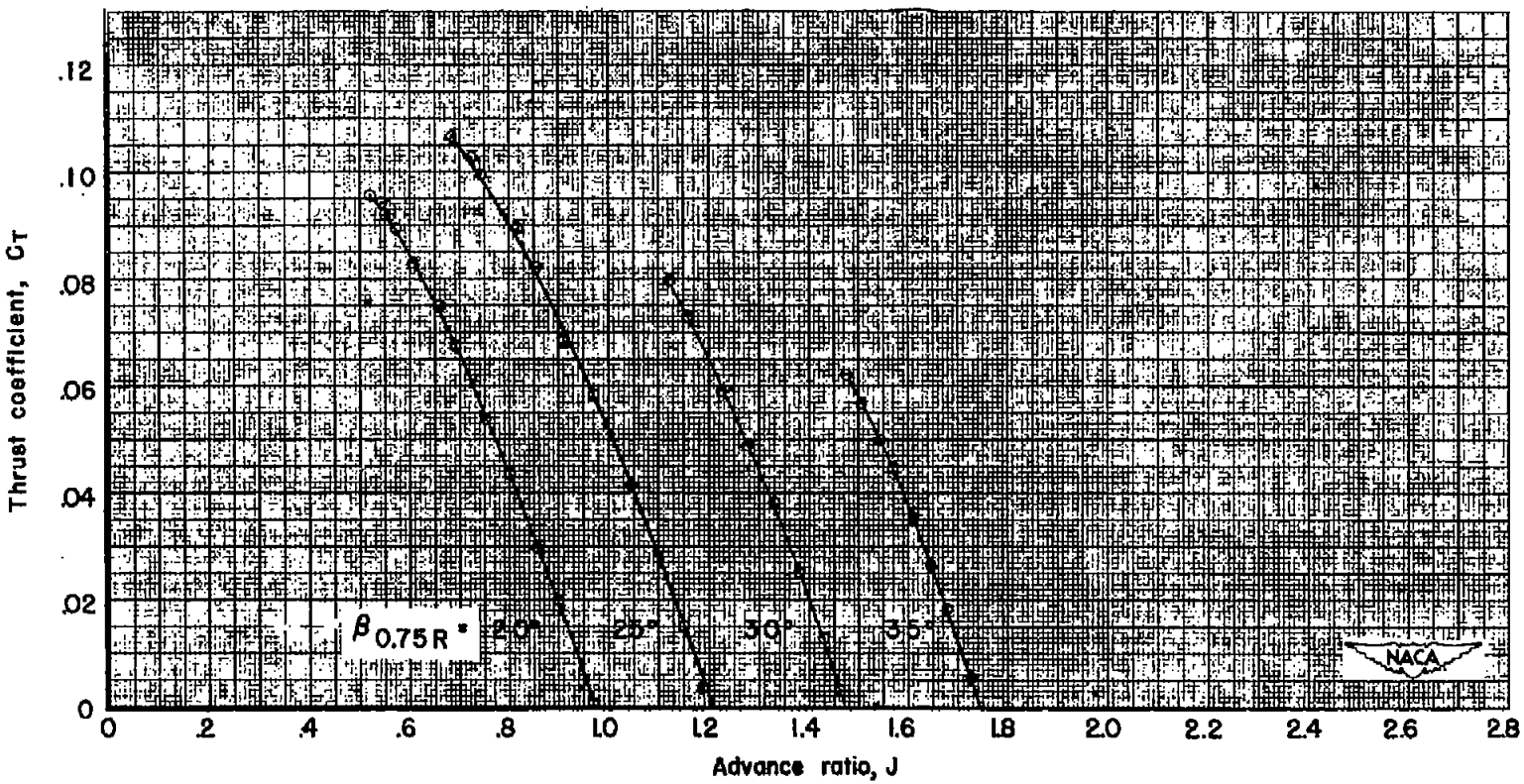

(a) Thrust coefficient.

Figure 10.- Characteristics of NACA 10-(4)(08)-03CY propeller. Rotational speed, 2000 rpm.

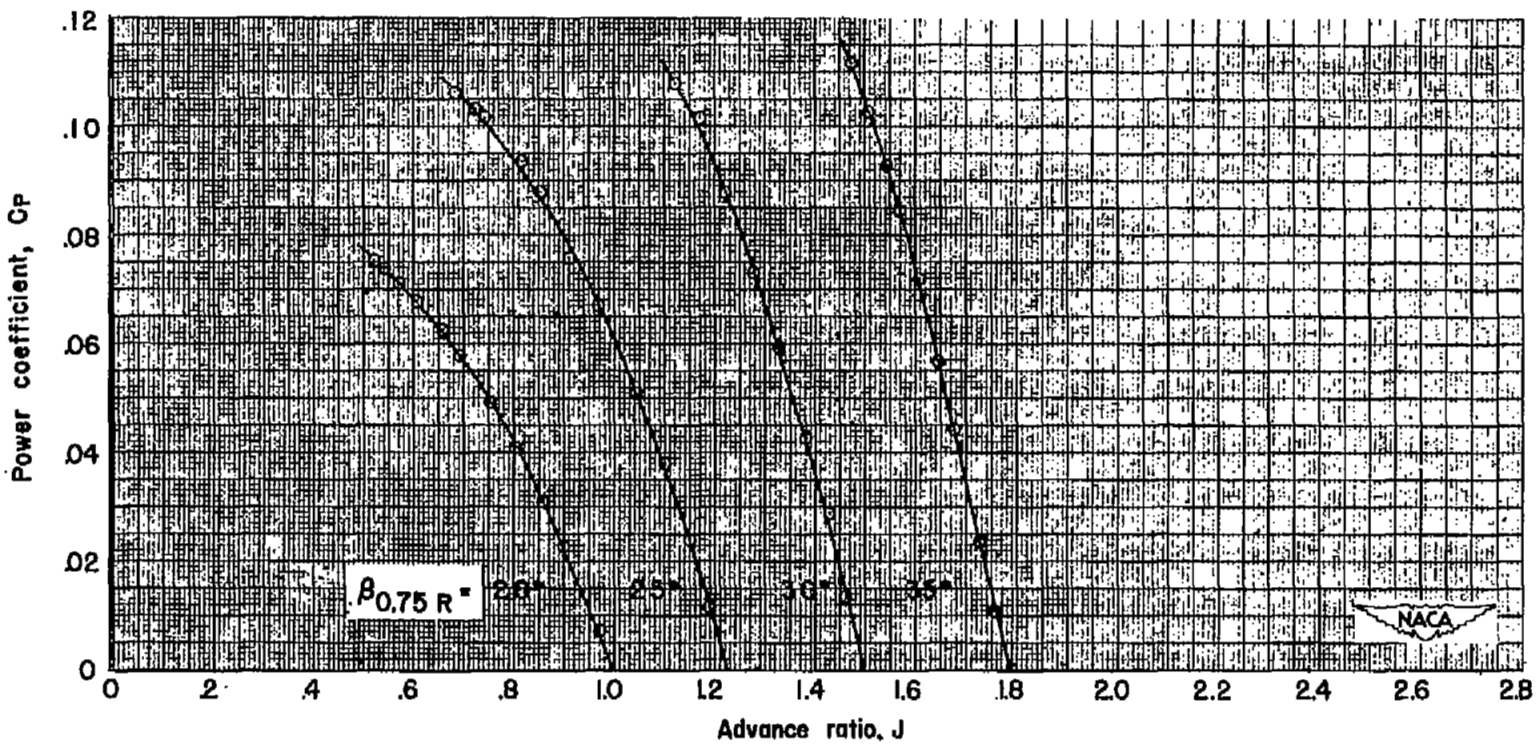

(b) Power coefficient.

Figure 10.- Continued. Rotational speed, 2000 rpm.

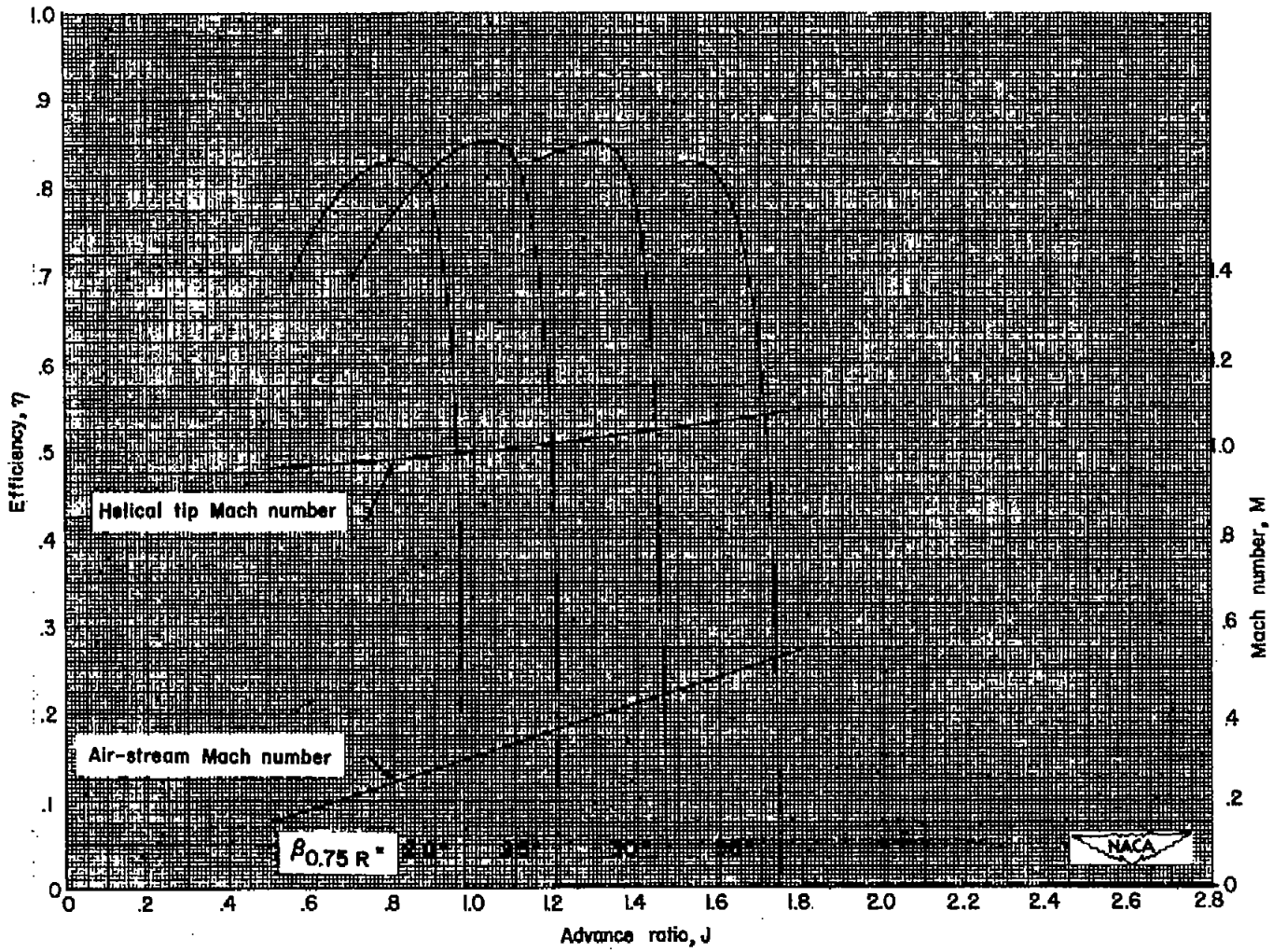

(c) Efficiency.

Figure 10.- Concluded. Rotational speed, 2000 rpm.

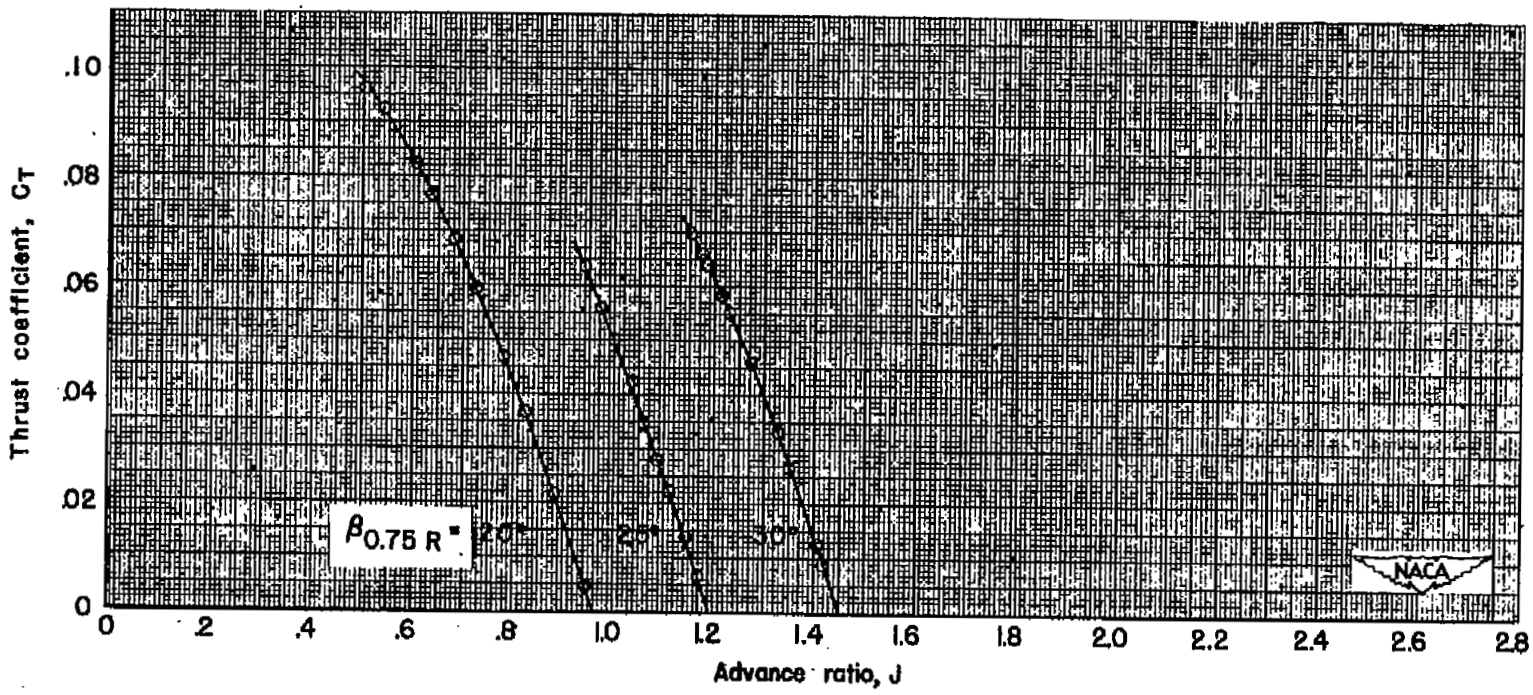

(a) Thrust coefficient.

Figure 11.- Characteristics of NACA 10-(4)(08)-03CY propeller. Rotational speed, 2160 rpm.

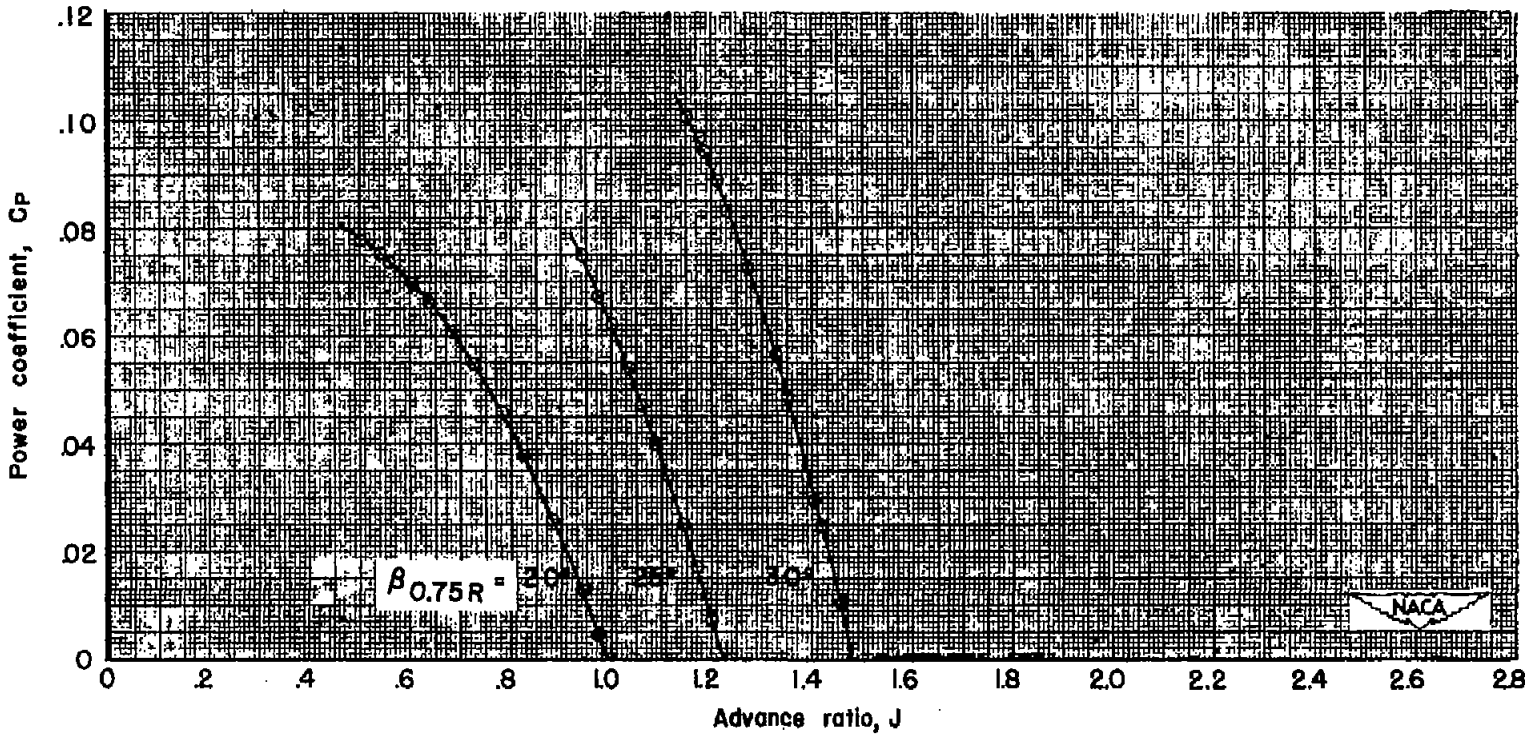

(b) Power coefficient.

Figure 11.- Continued. Rotational speed, 2160 rpm.

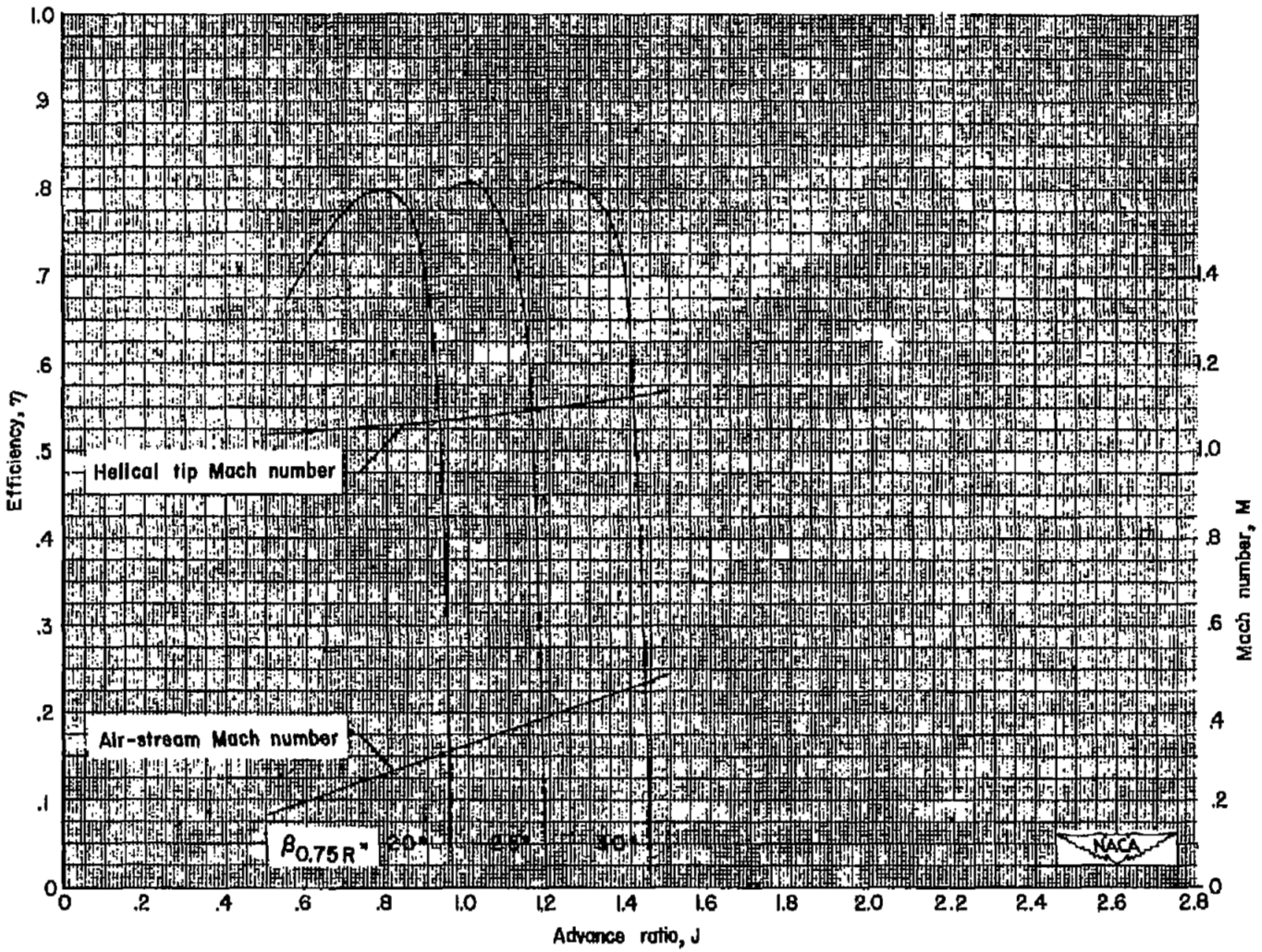

(c) Efficiency.

Figure 11.- Concluded. Rotational speed, 2160 rpm.

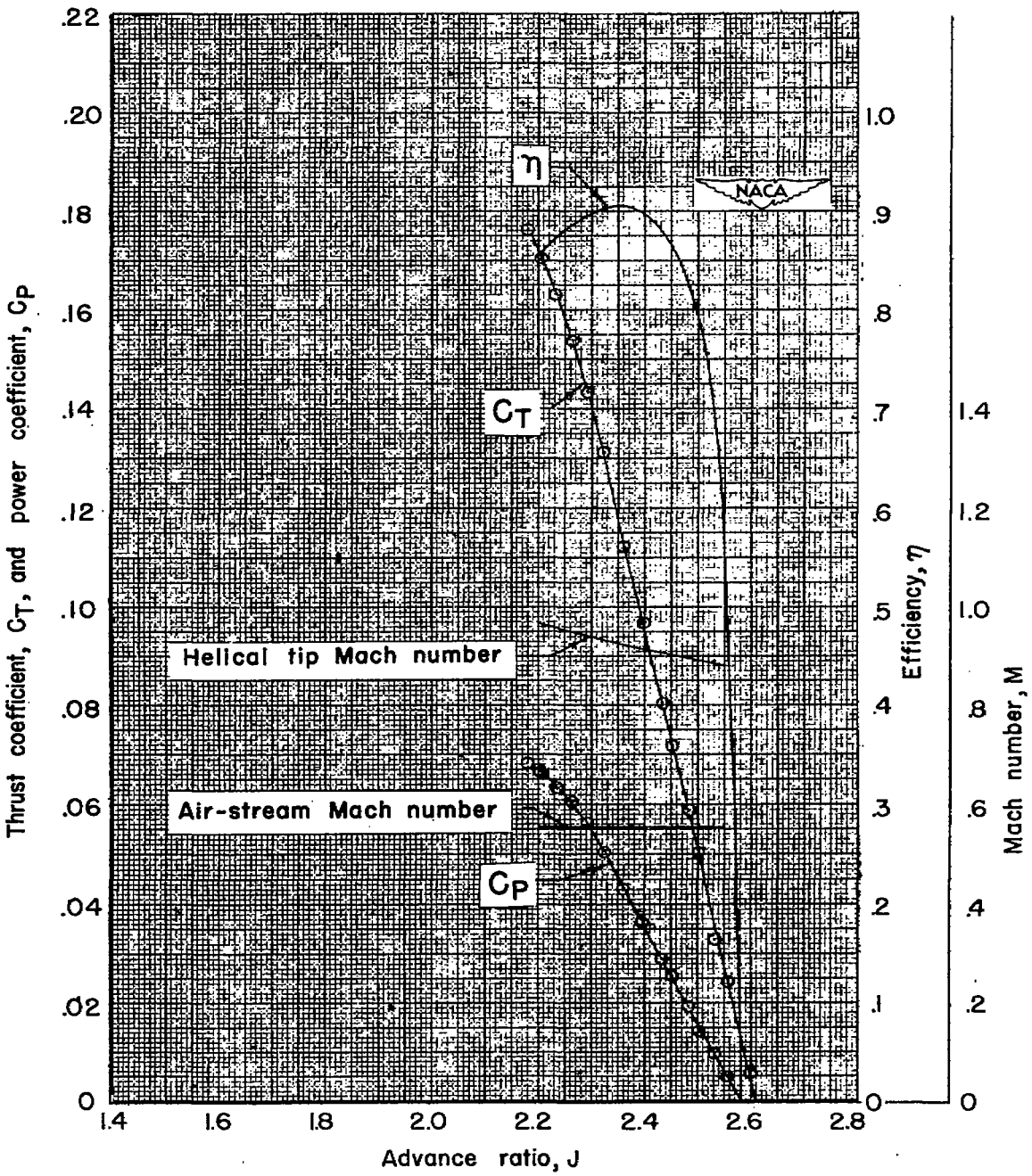

(a) Air-stream Mach number at maximum efficiency, 0.555.

Figure 12.- Characteristics of NACA 10-(4)(08)-03CY propeller at high forward speeds. $\beta_{0.75R} = 45^{\circ}$.

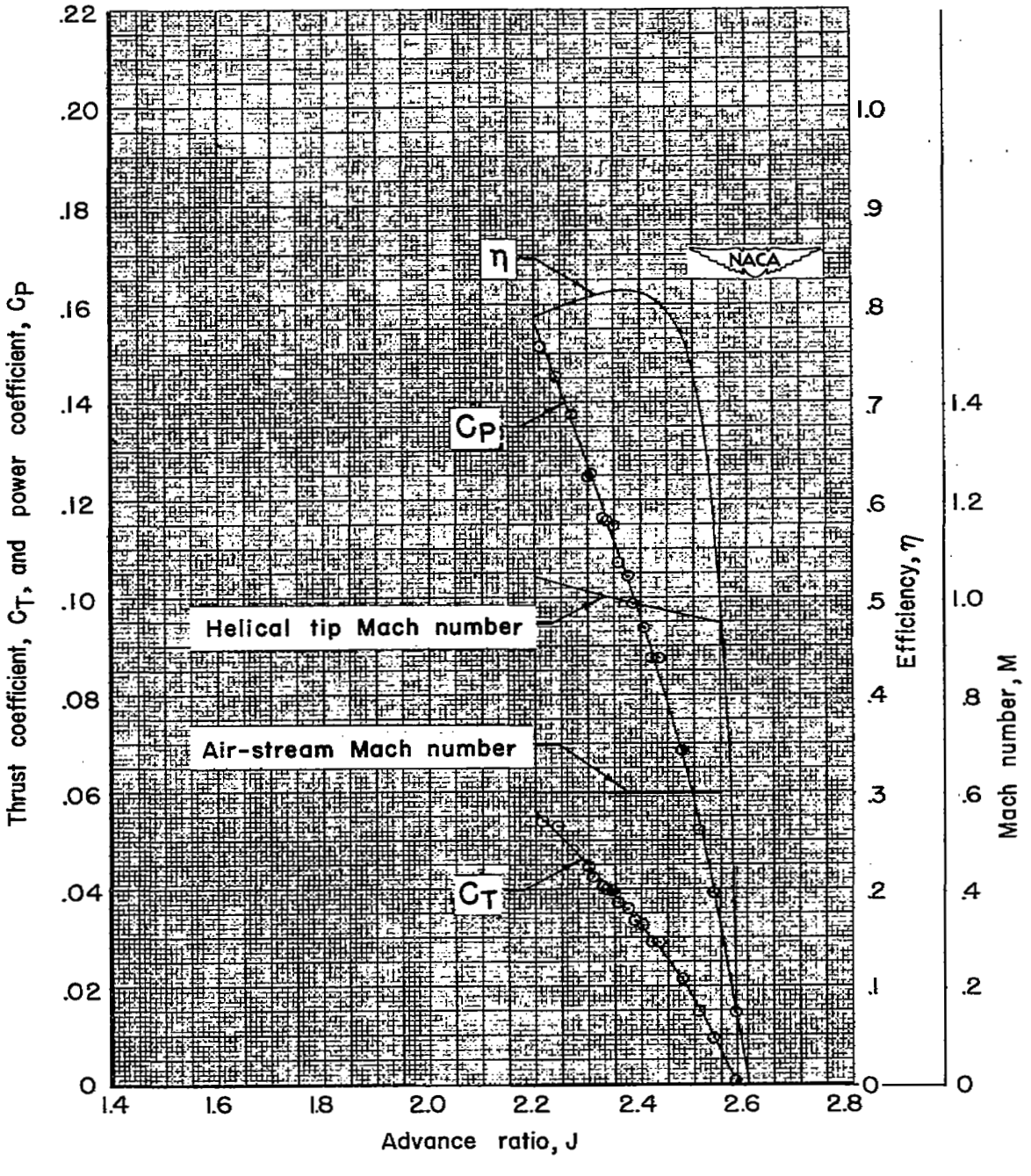

(b) Air-stream Mach number at maximum efficiency, 0.600.

Figure 12.- Continued.

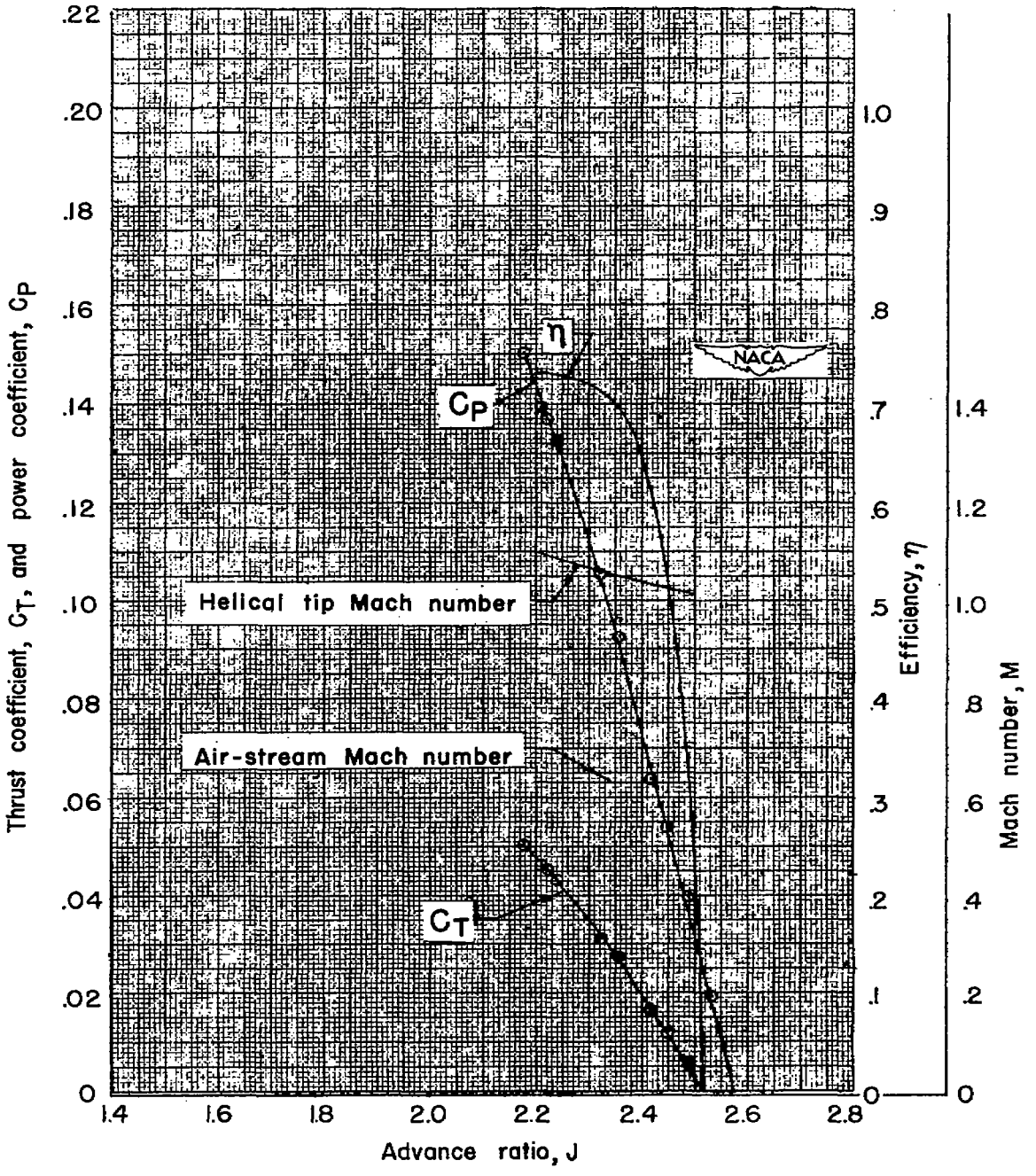

(c) Air-stream Mach number at maximum efficiency, 0.631.

Figure 12.- Continued.

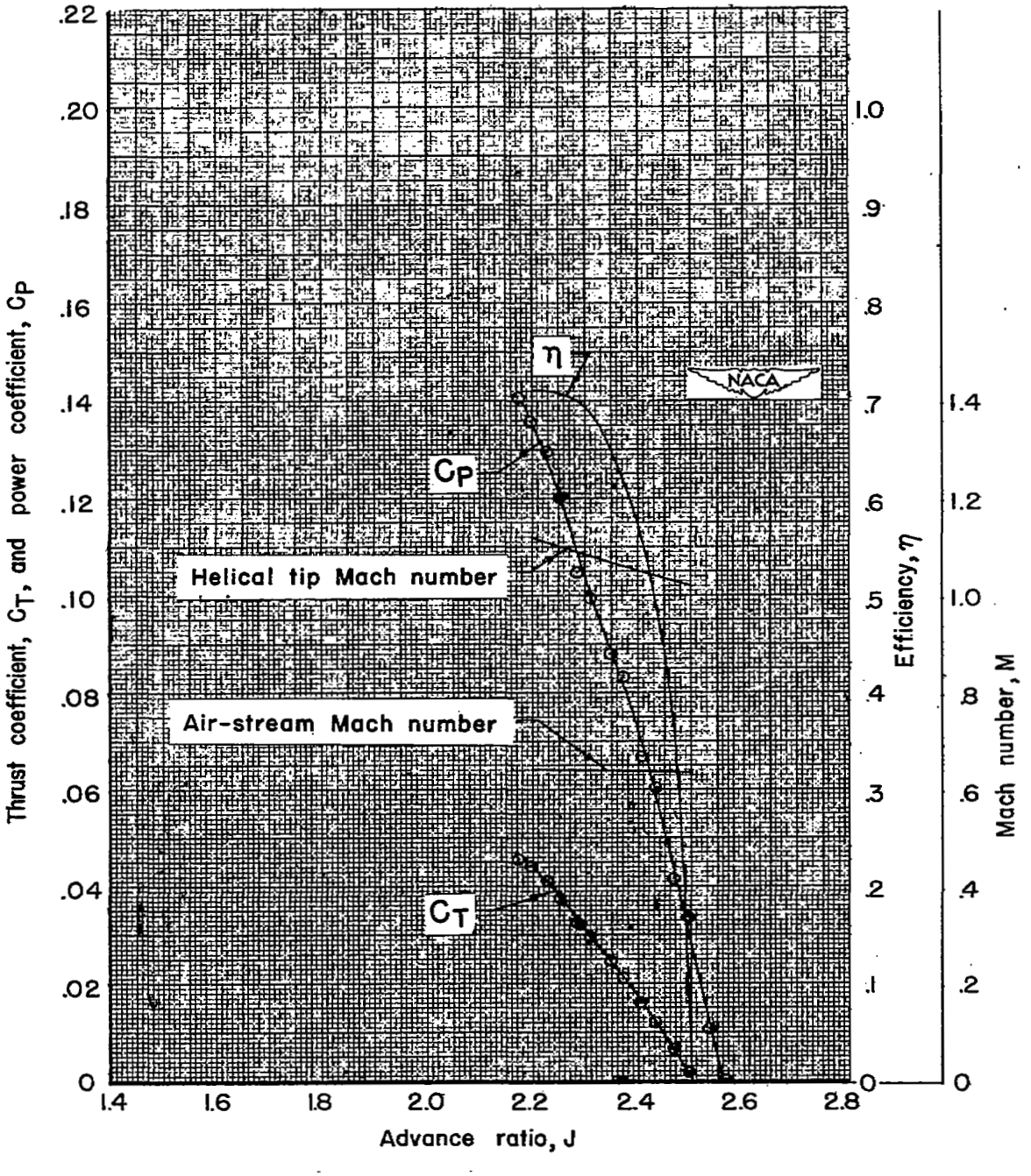

(d) Air-stream Mach number at maximum efficiency, 0.642.

Figure 12.- Concluded.

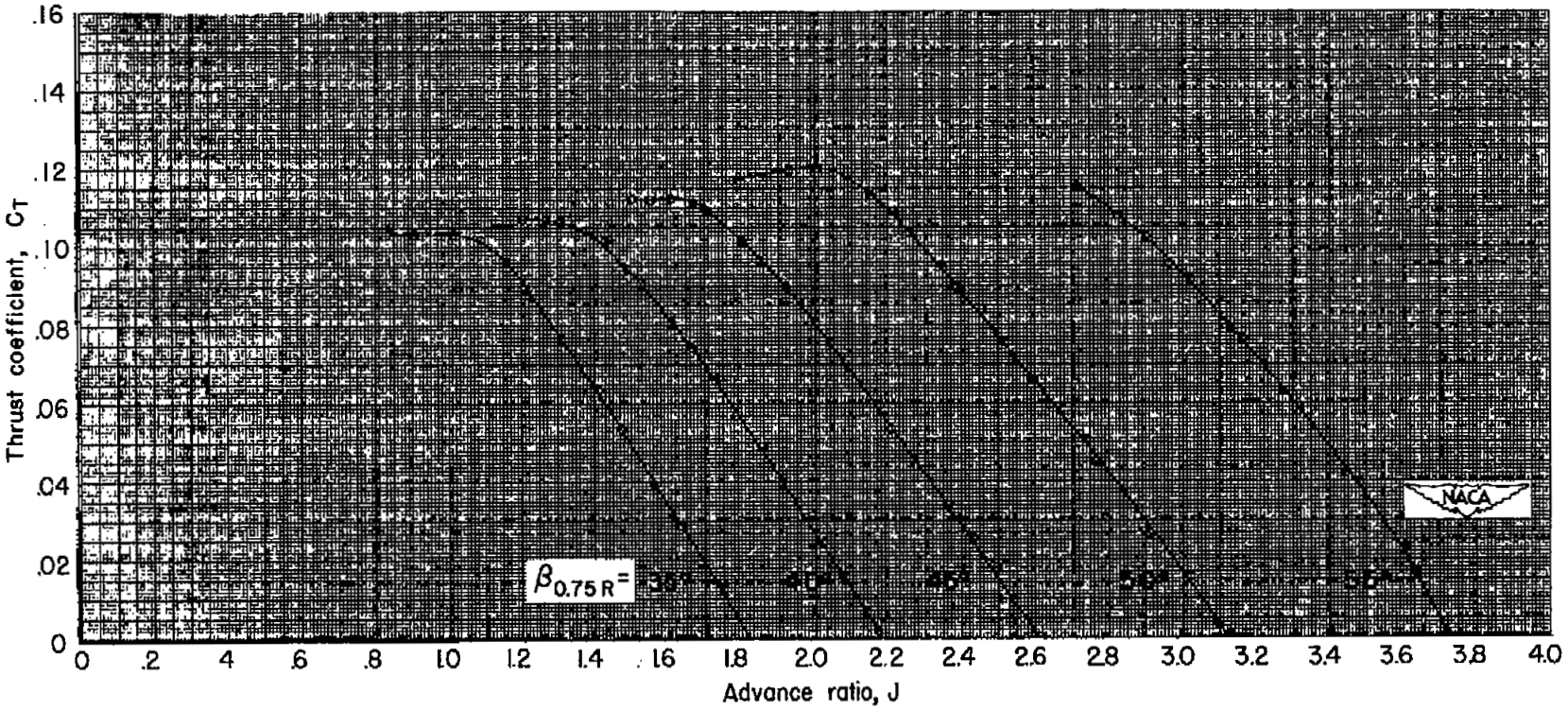

(a) Thrust coefficient.

Figure 13.- Characteristics of NACA 10-(4)(08)-03RCY propeller. Rotational speed, 1140 rpm.

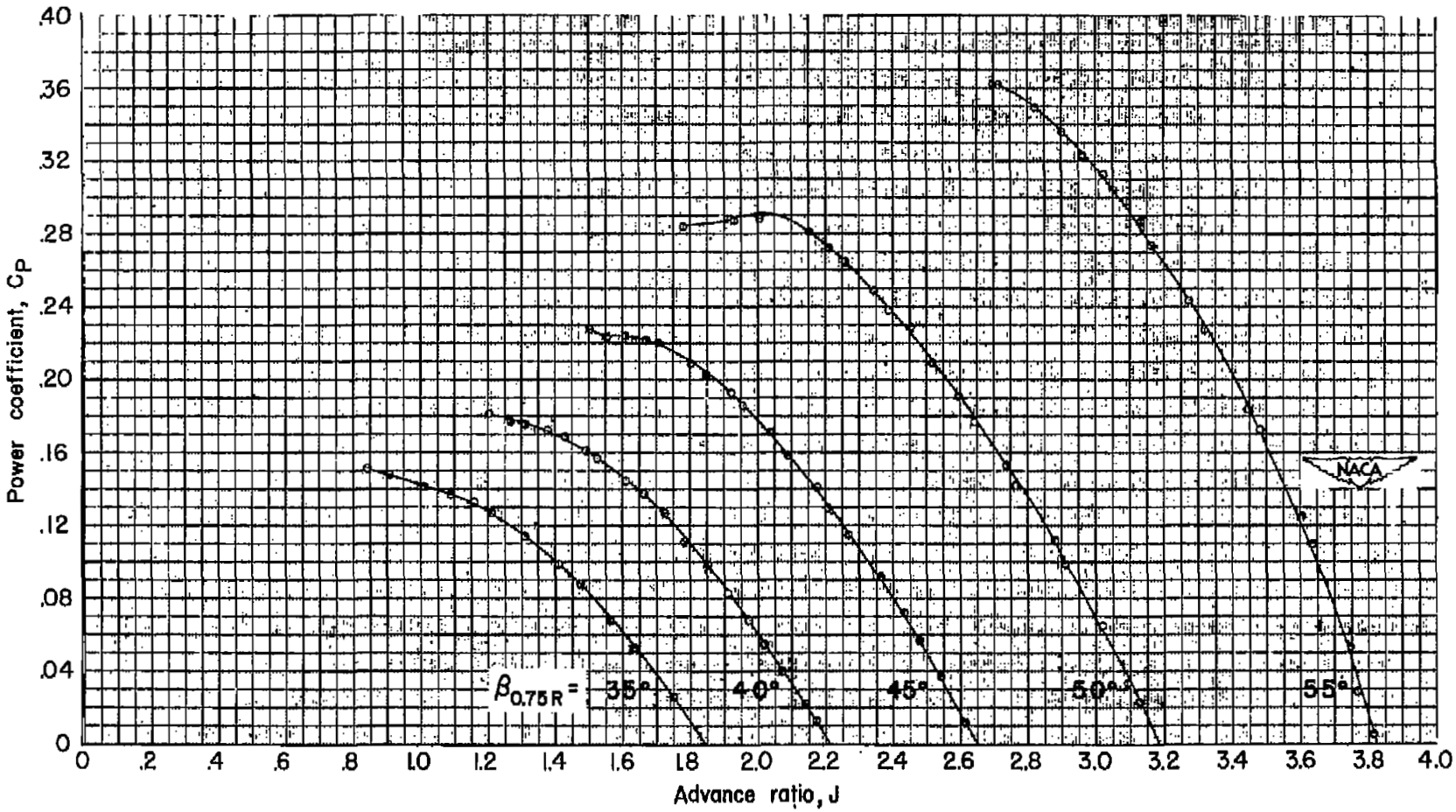

(b) Power coefficient.

Figure 13.- Continued. Rotational speed, 1140 rpm.

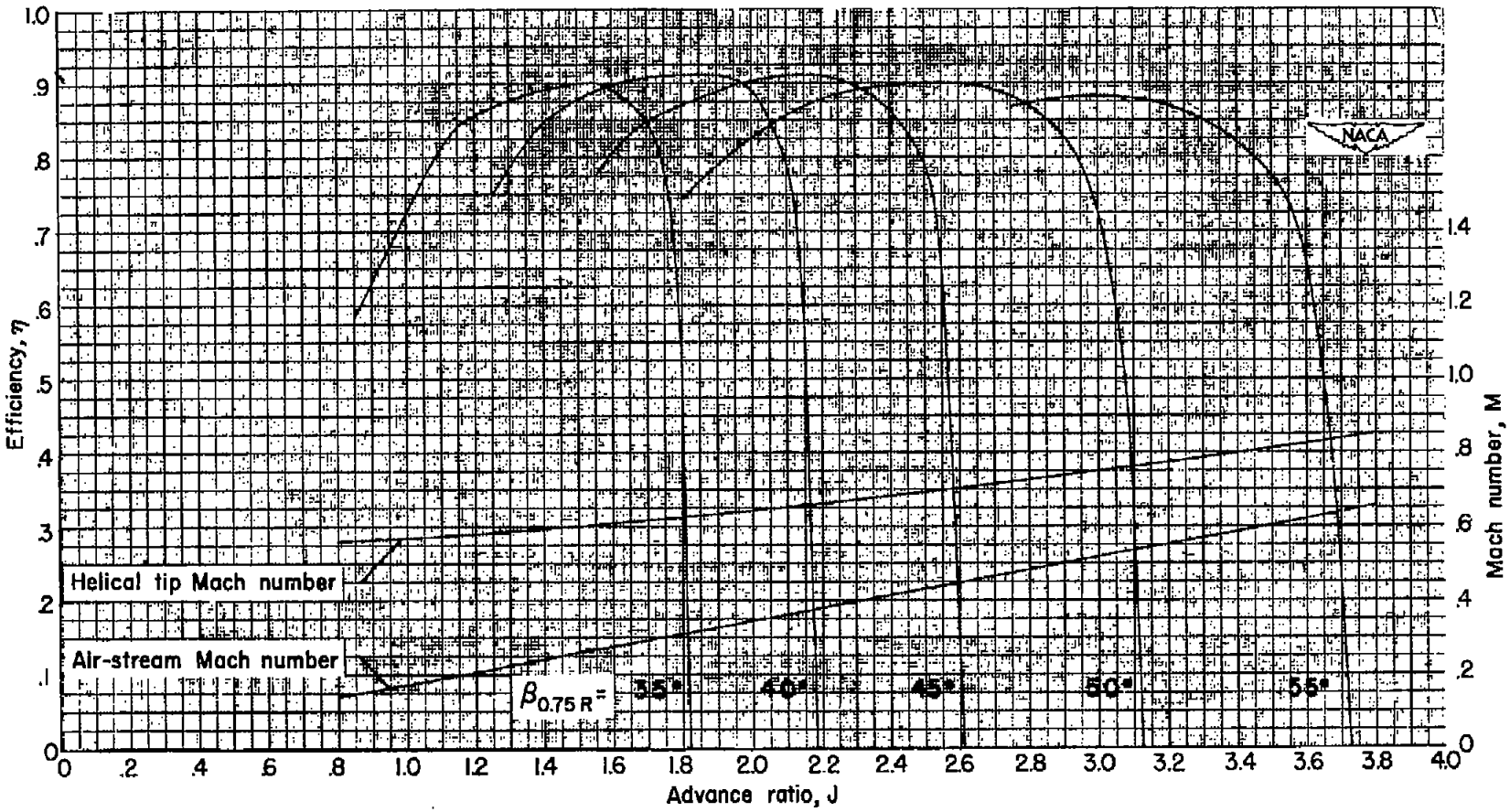

(c) Efficiency.

Figure 13.- Concluded. Rotational speed, 1140 rpm.

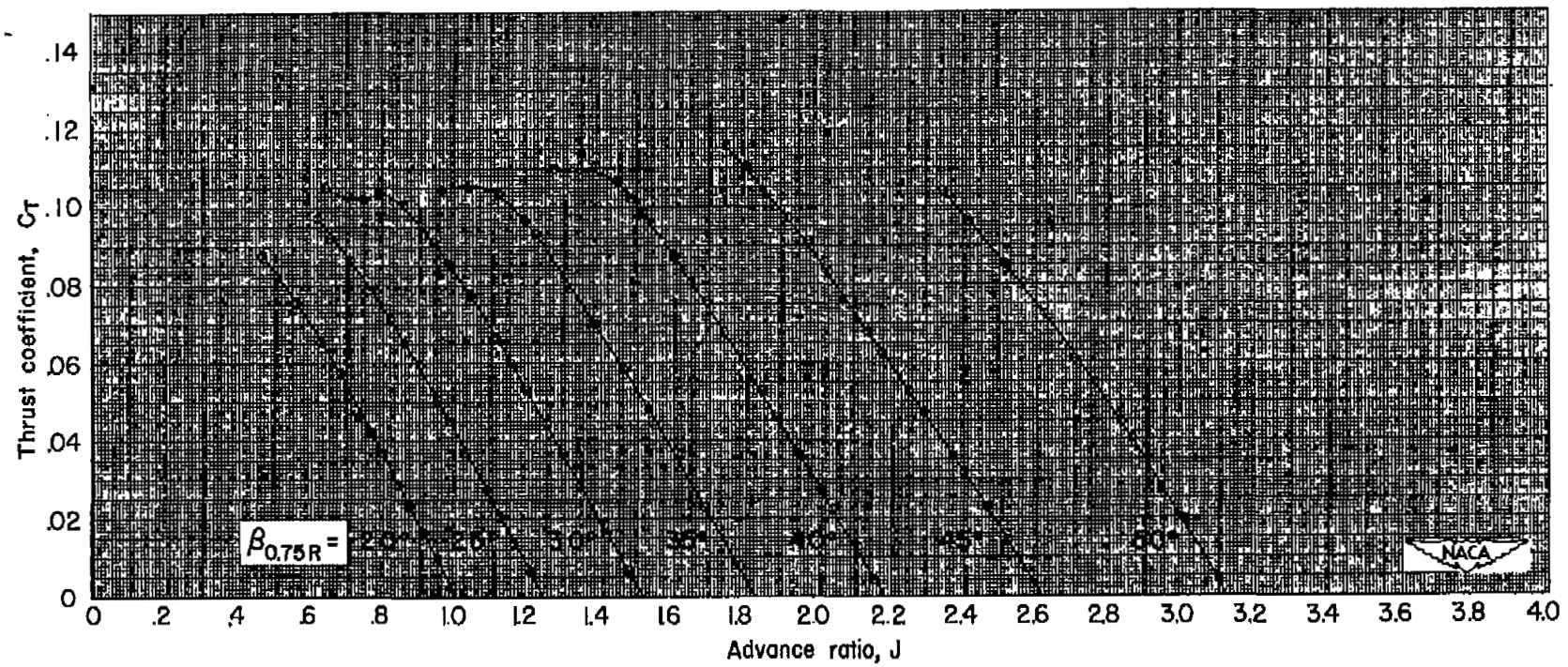

(a) Thrust coefficient.

Figure 14.- Characteristics of NACA 10-(4)(08)-03RCY propeller. Rotational speed, 1350 rpm.

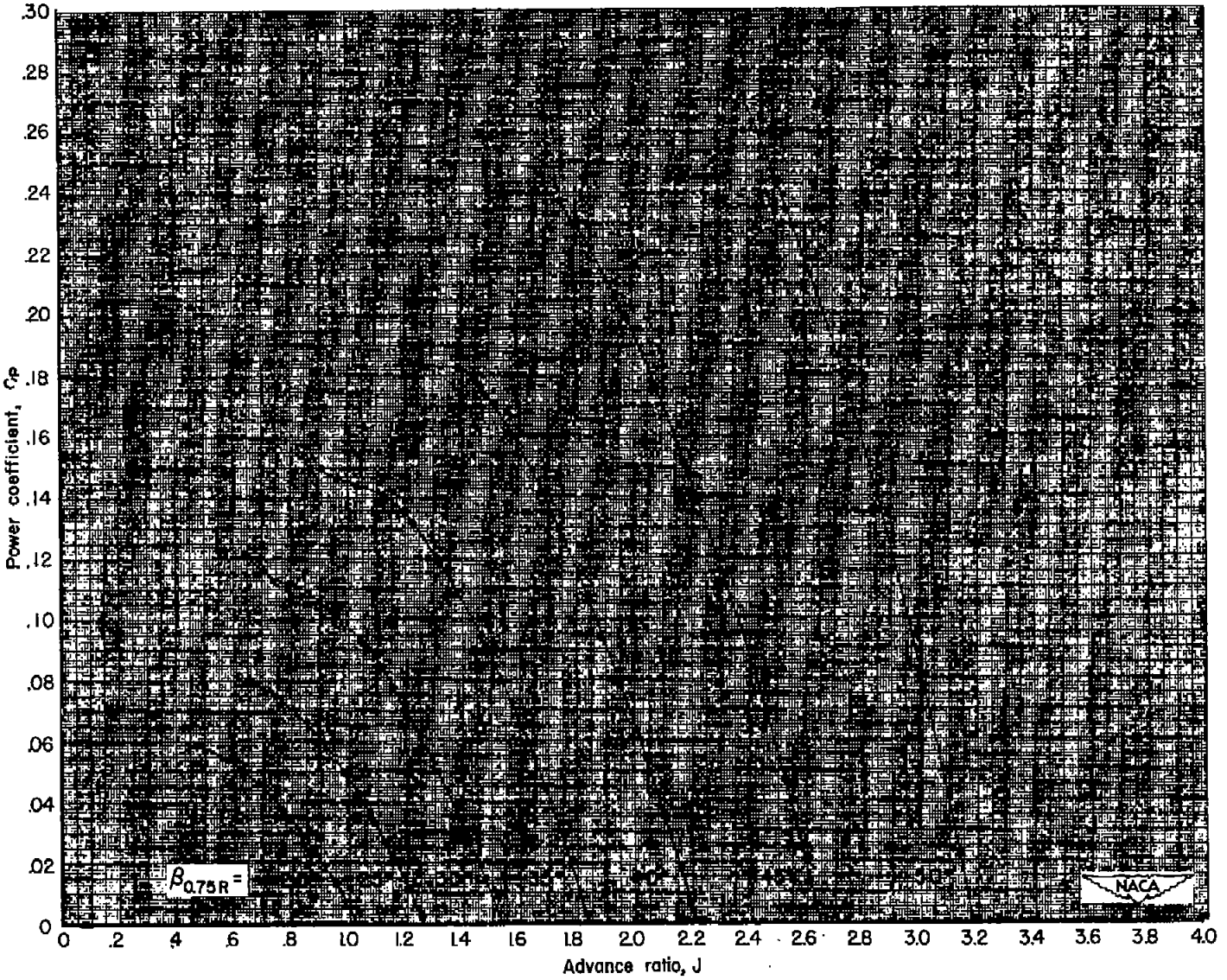

(b) Power coefficient.

Figure 14.- Continued. Rotational speed, 1350 rpm.

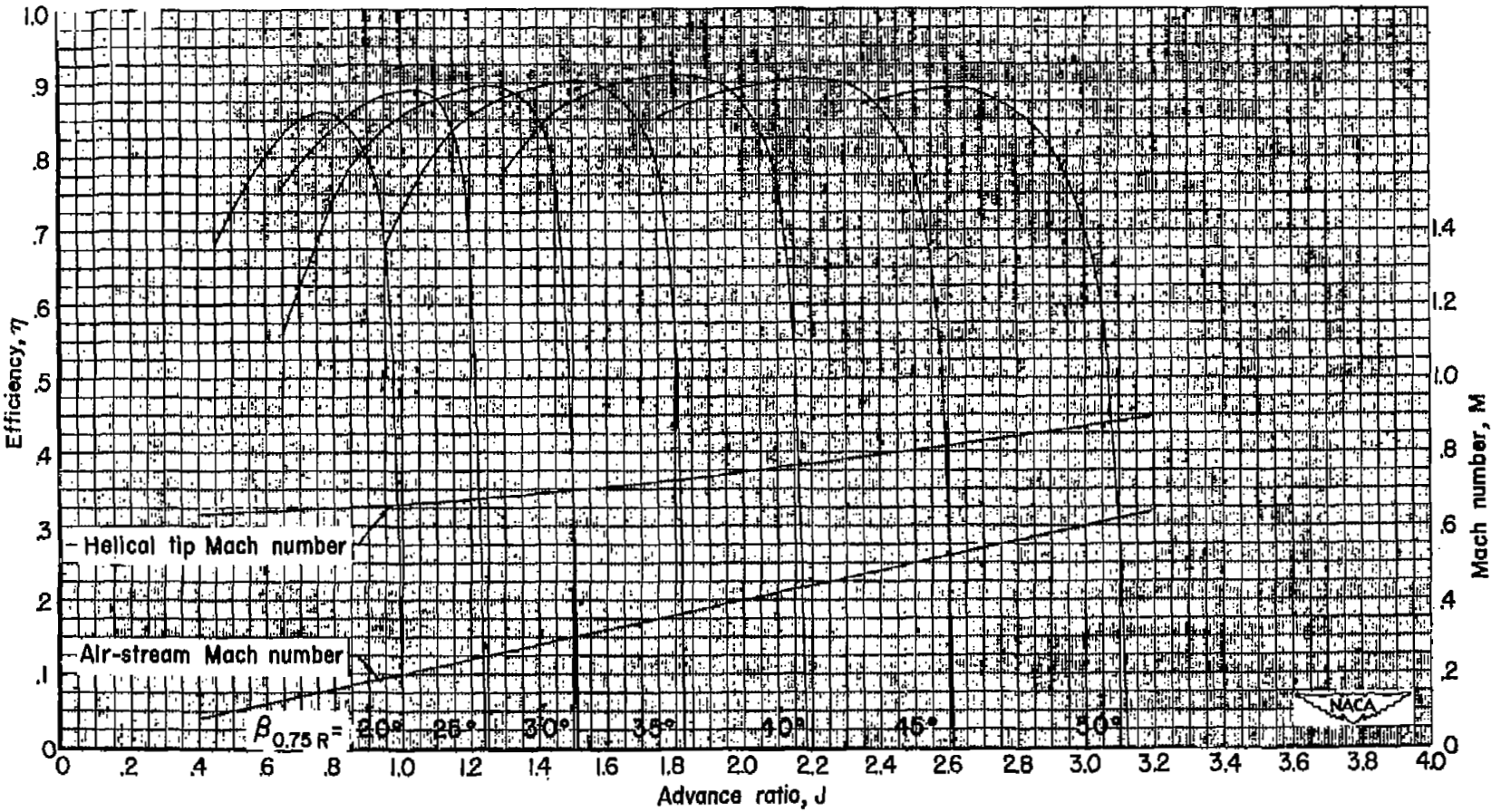

(c) Efficiency.

Figure 14.- Concluded. Rotational speed, 1350 rpm.

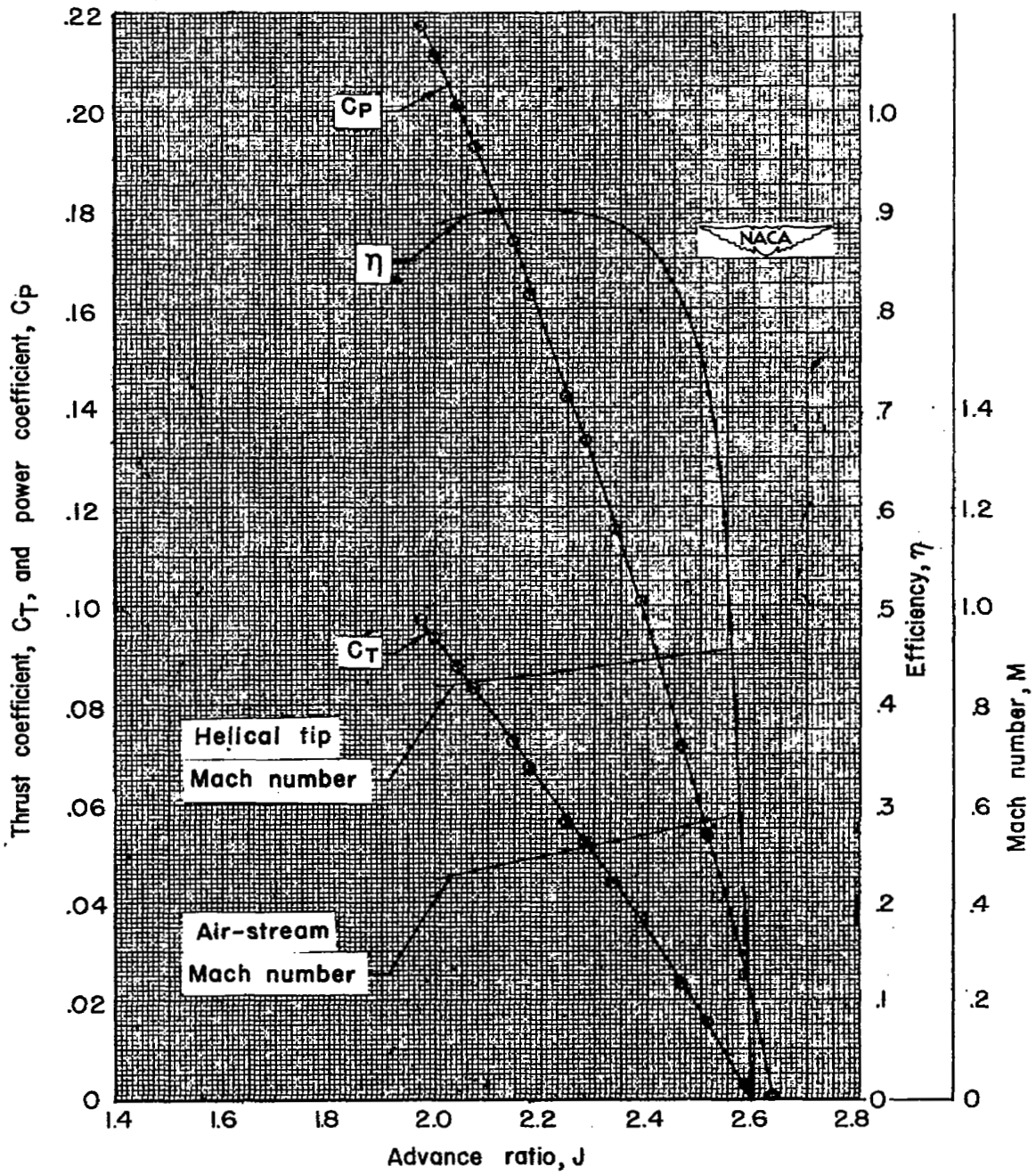

Figure 15.- Characteristics of NACA 10-(4)(08)-03RCY propeller. Rotational speed, 1500 rpm. $\beta_{0.75R} = 45^{\circ}$.

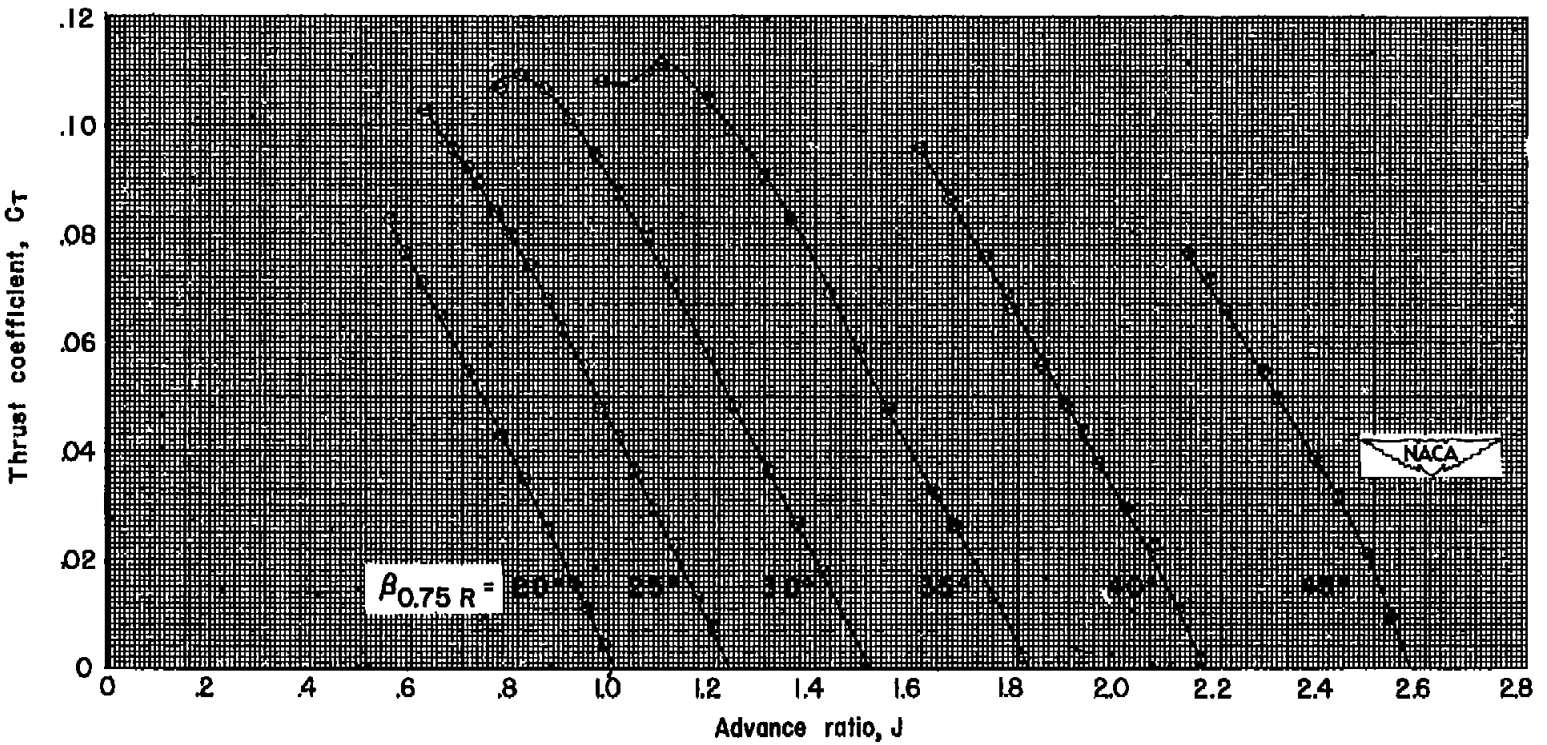

(a) Thrust coefficient.

Figure 16.- Characteristics of NACA 10-(4)(08)-03RCY propeller. Rotational speed, 1600 rpm.

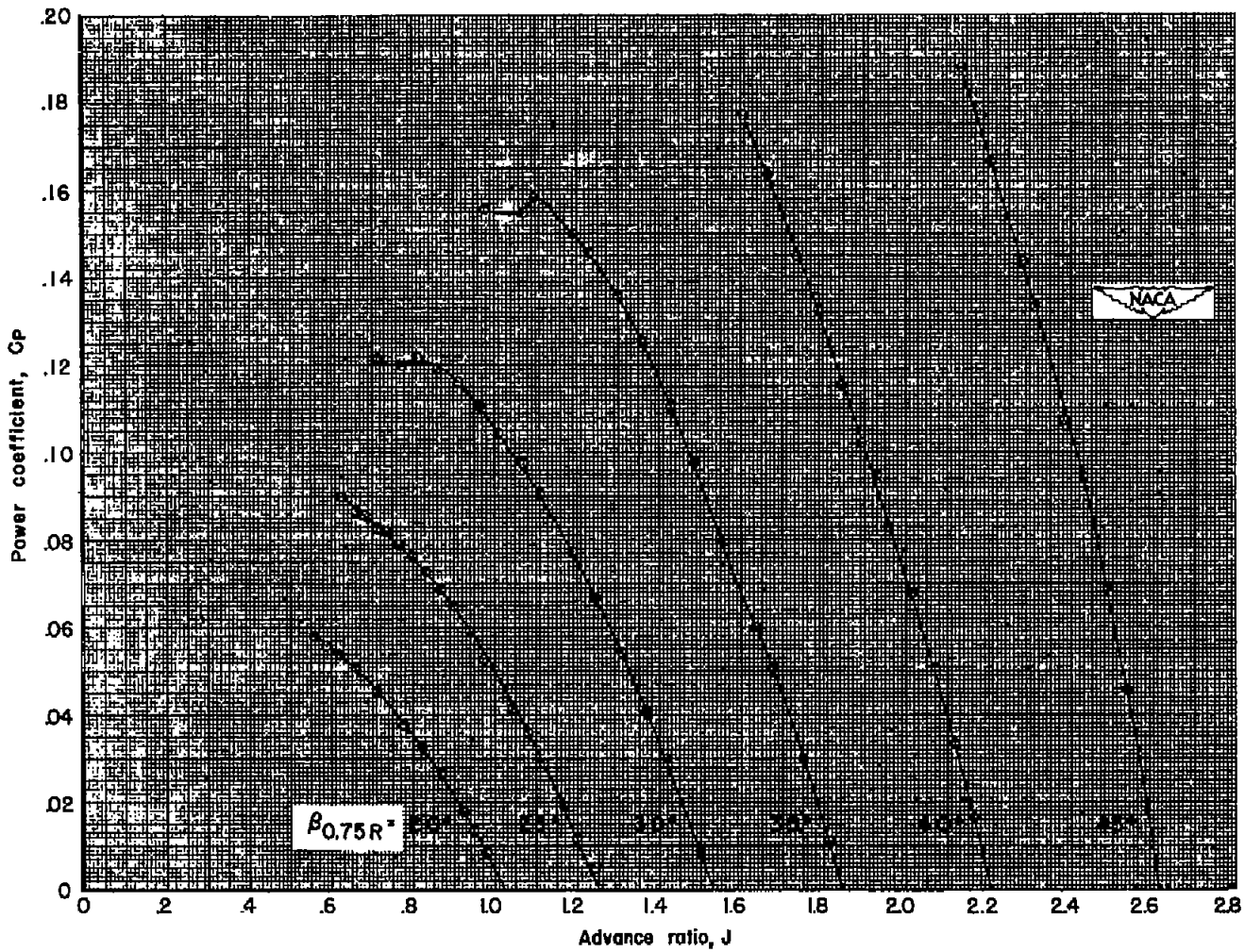

(b) Power coefficient.

Figure 16.- Continued. Rotational speed, 1600 rpm.

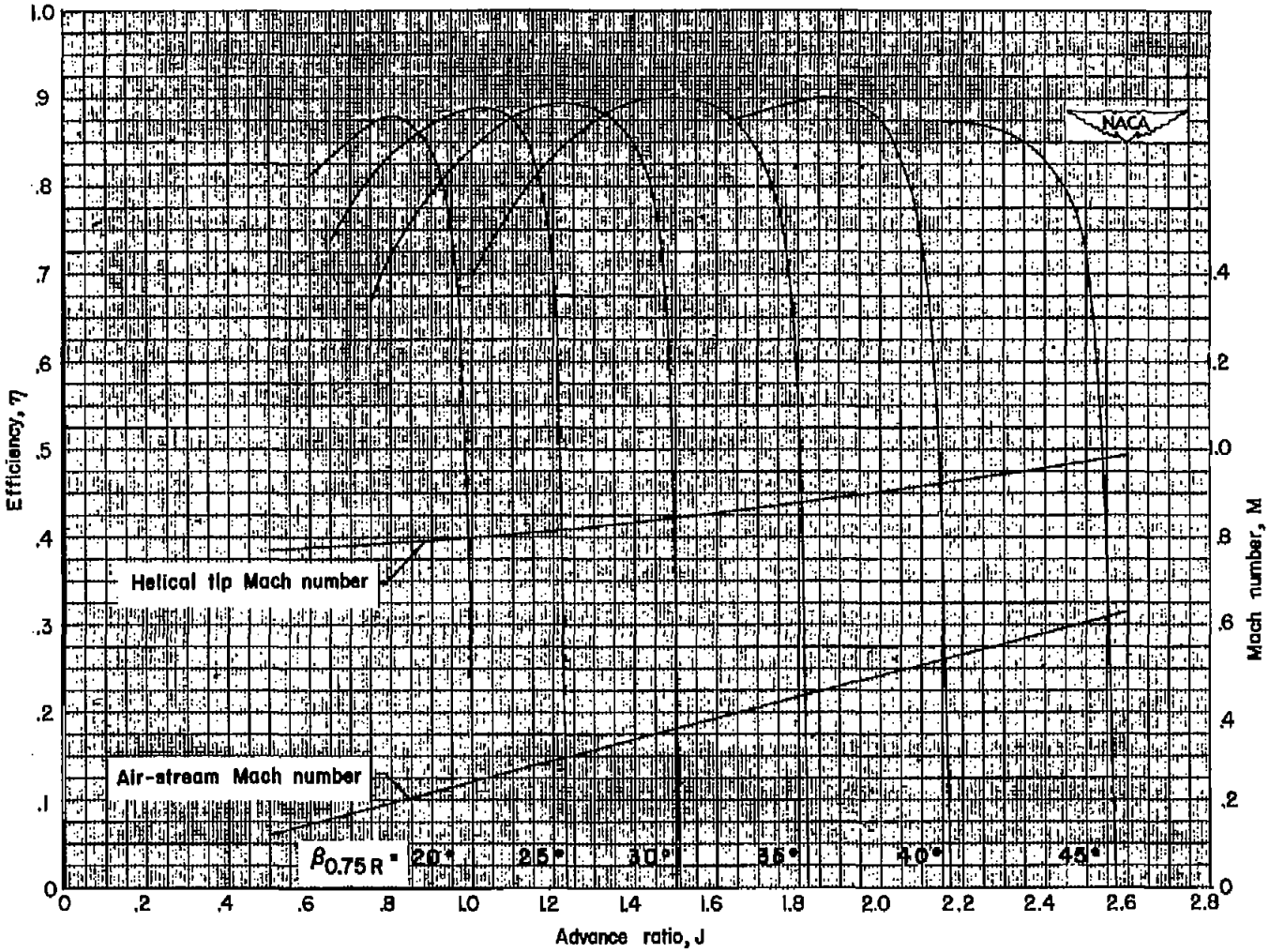

(c) Efficiency.

Figure 16.- Concluded. Rotational speed, 1600 rpm.

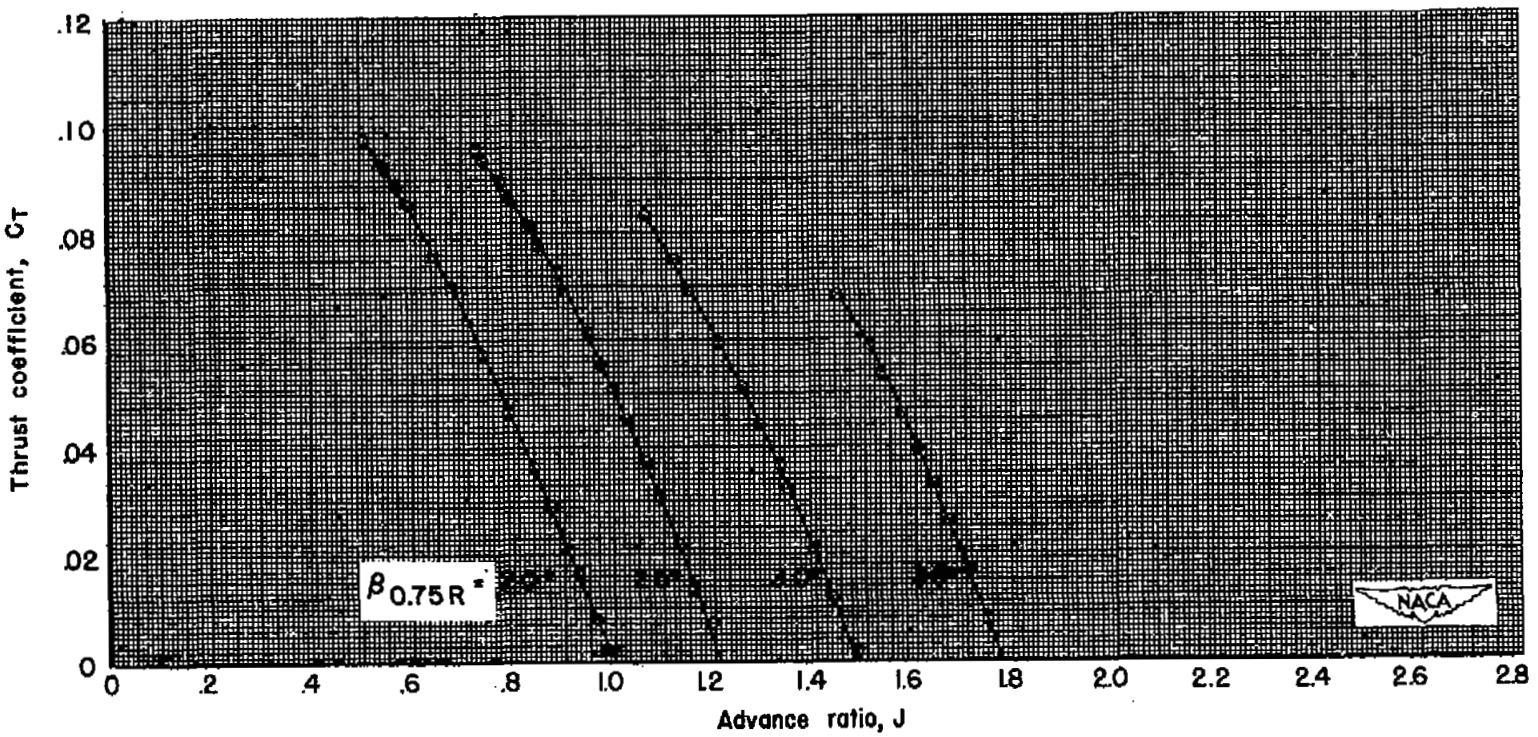

(a) Thrust coefficient.

Figure 17.- Characteristics of NACA 10-(4)(08)-03RCY propeller. Rotational speed, 2000 rpm.

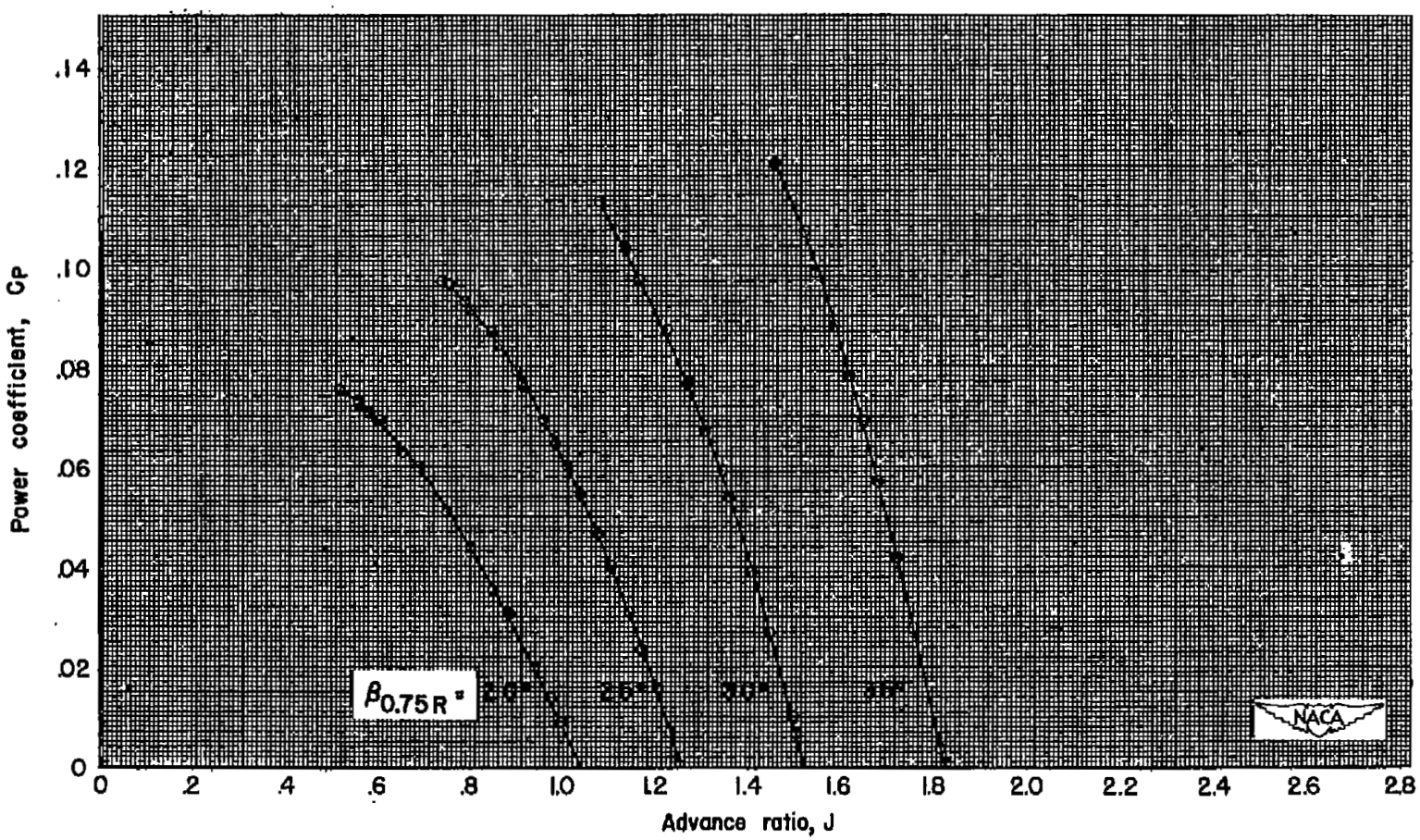

(b) Power coefficient.

Figure 17.- Continued. Rotational speed, 2000 rpm.

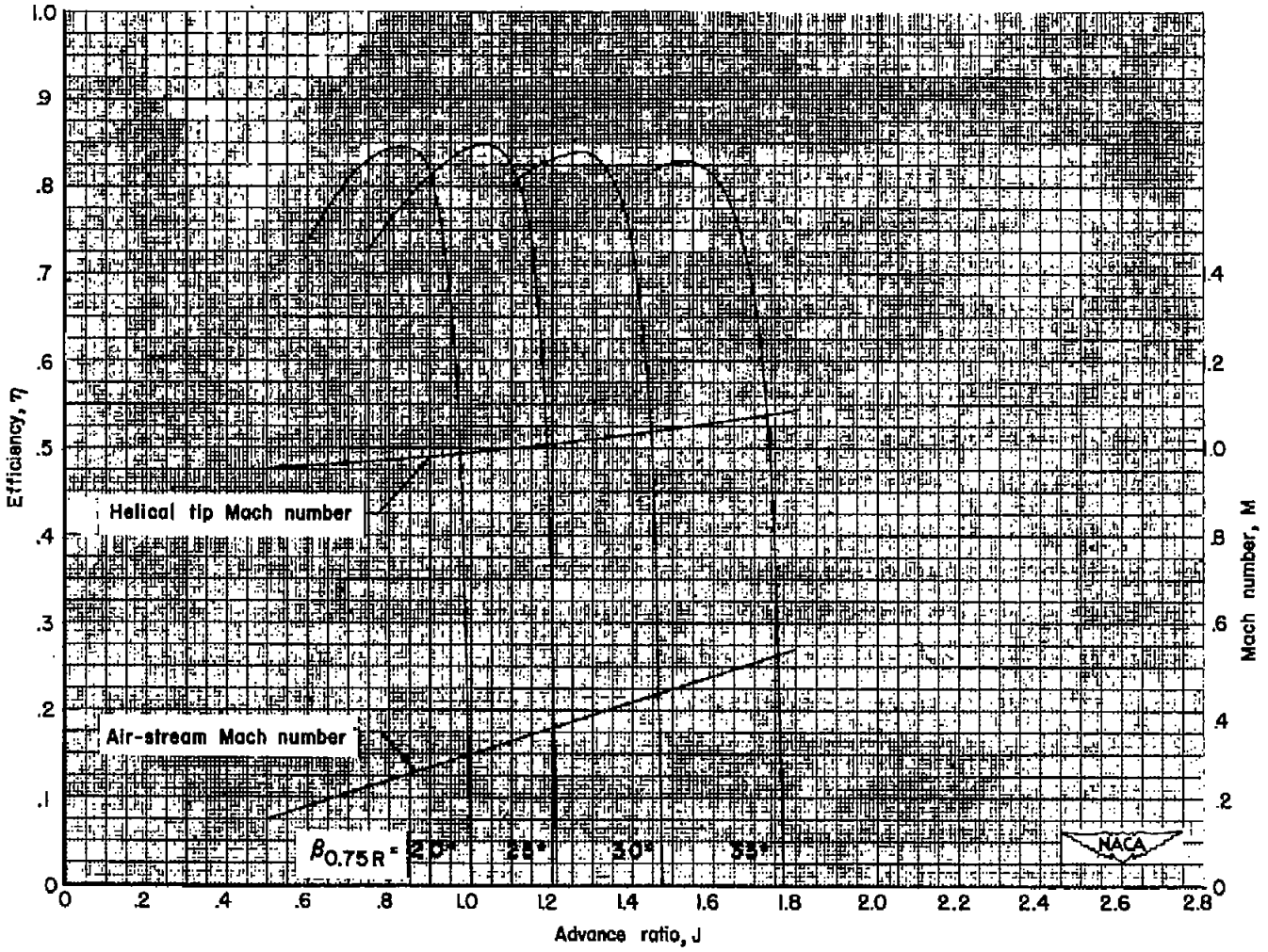

(c) Efficiency.

Figure 17.- Concluded. Rotational speed, 2000 rpm.

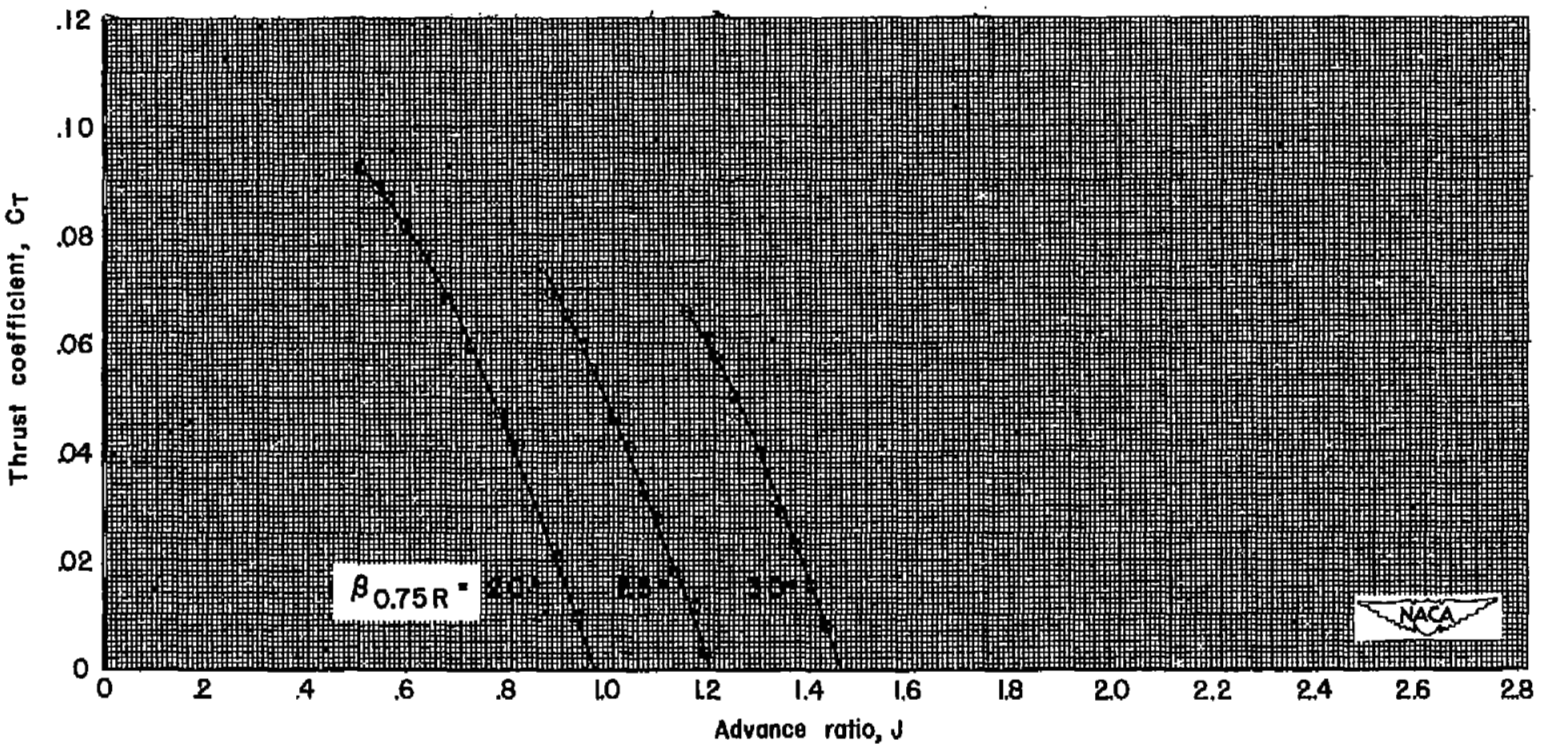

(a) Thrust coefficient.

Figure 18.- Characteristics of NACA 10-(4)(08)-03RCY propeller. Rotational speed, 2160 rpm.

NACA – Digidocs

Document processing error

Unreadable tiff image

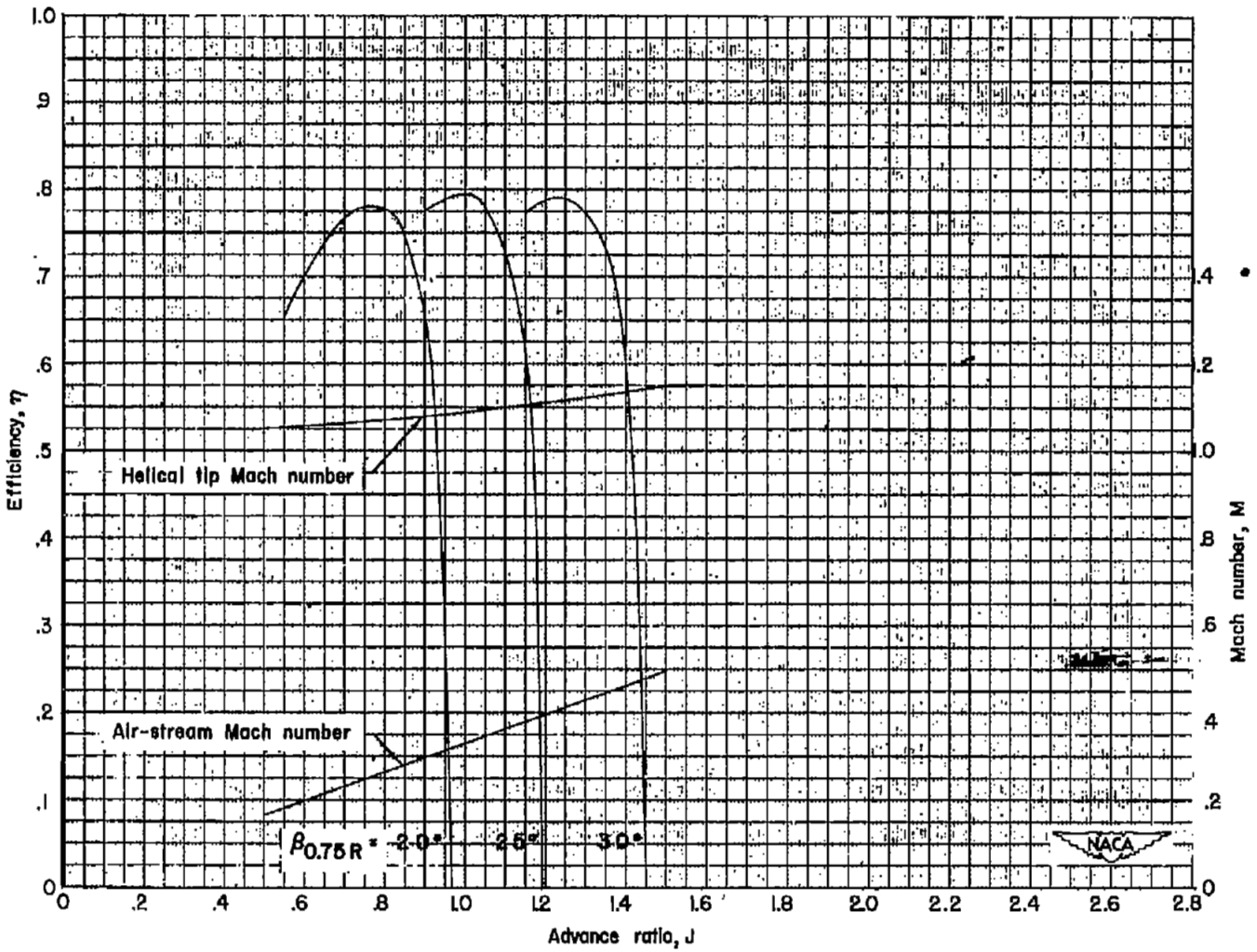

(c) Efficiency.

Figure 18.- Concluded. Rotational speed, 2160 rpm.

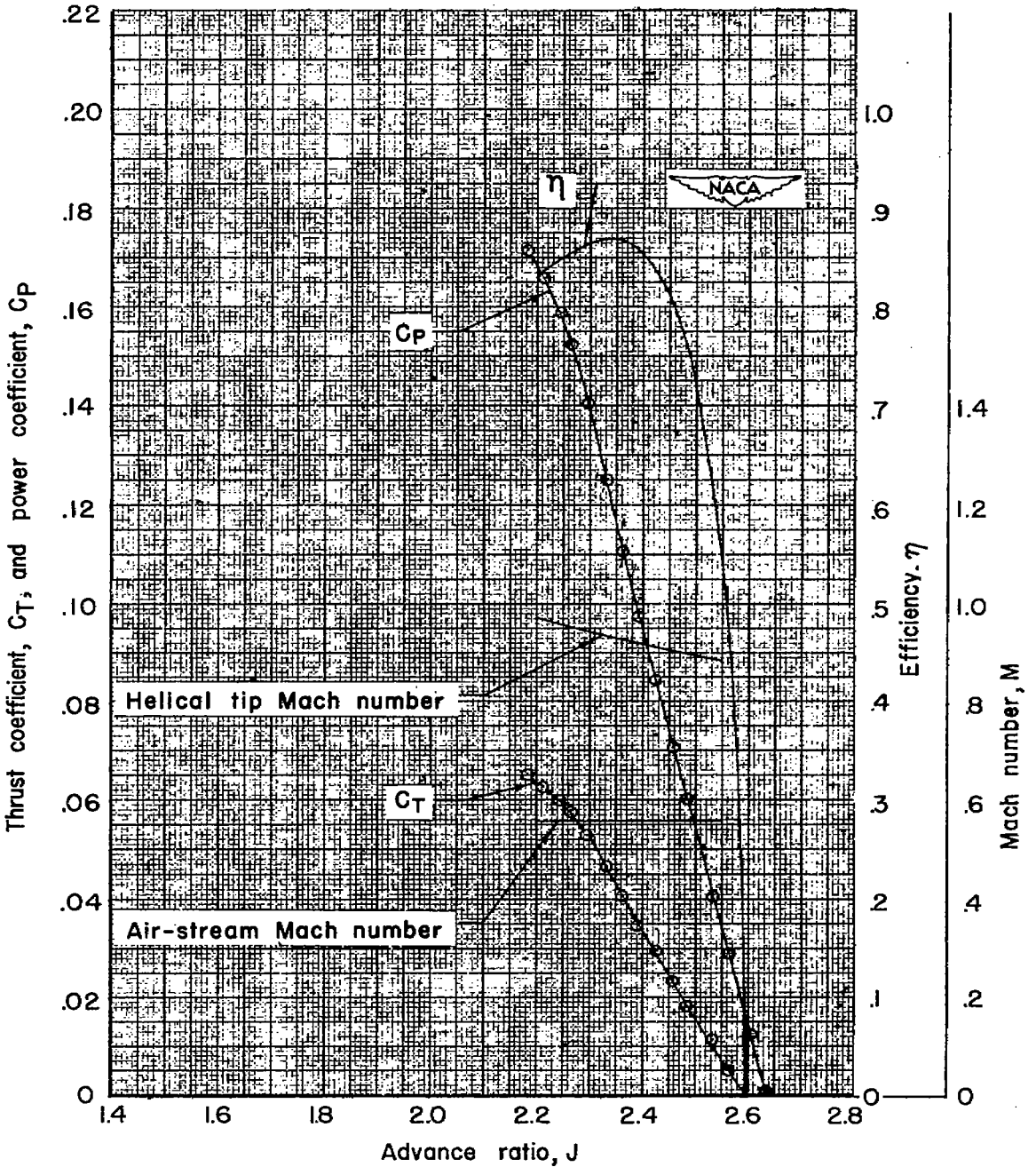

(a) Air-stream Mach number at maximum efficiency, 0.558.

Figure 19.- Characteristics of NACA 10-(4)(08)-03RCY propeller at high forward speeds. $\beta_{0.75R} = 45^{\circ}$.

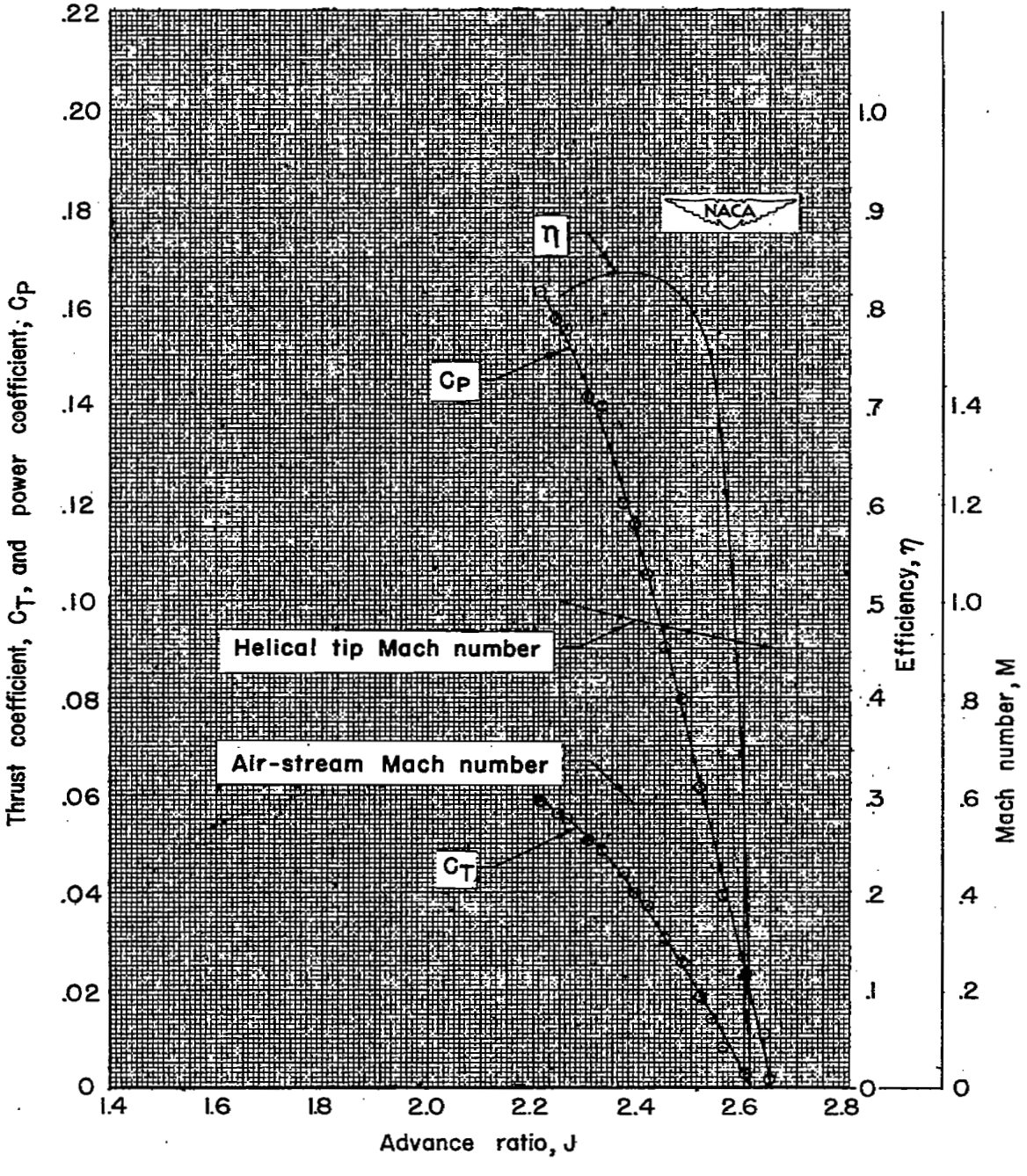

(b) Air-stream Mach number at maximum efficiency, 0.580.

Figure 19.- Continued.

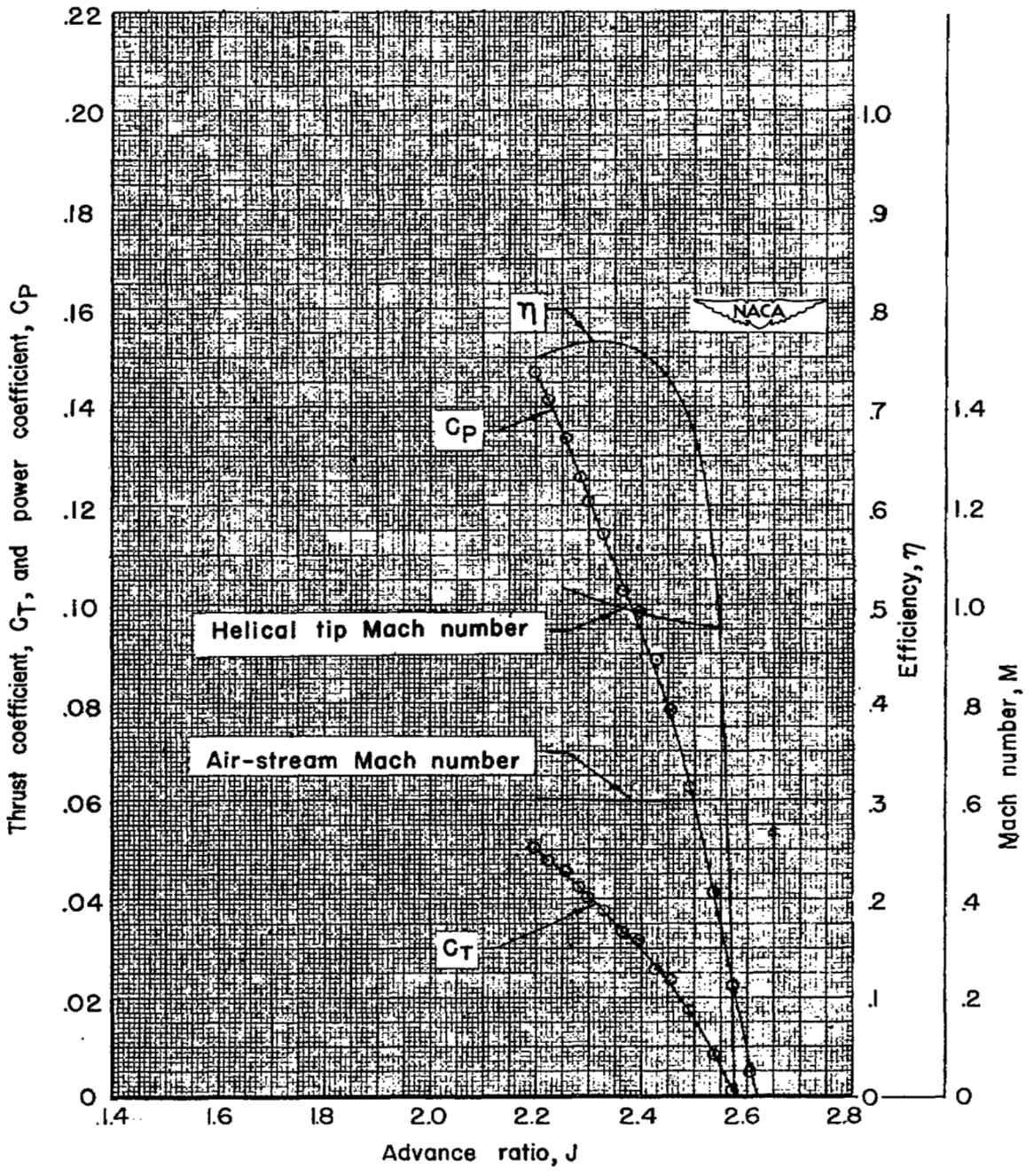

(c) Air-stream Mach number at maximum efficiency, 0.600.

Figure 19.- Continued.

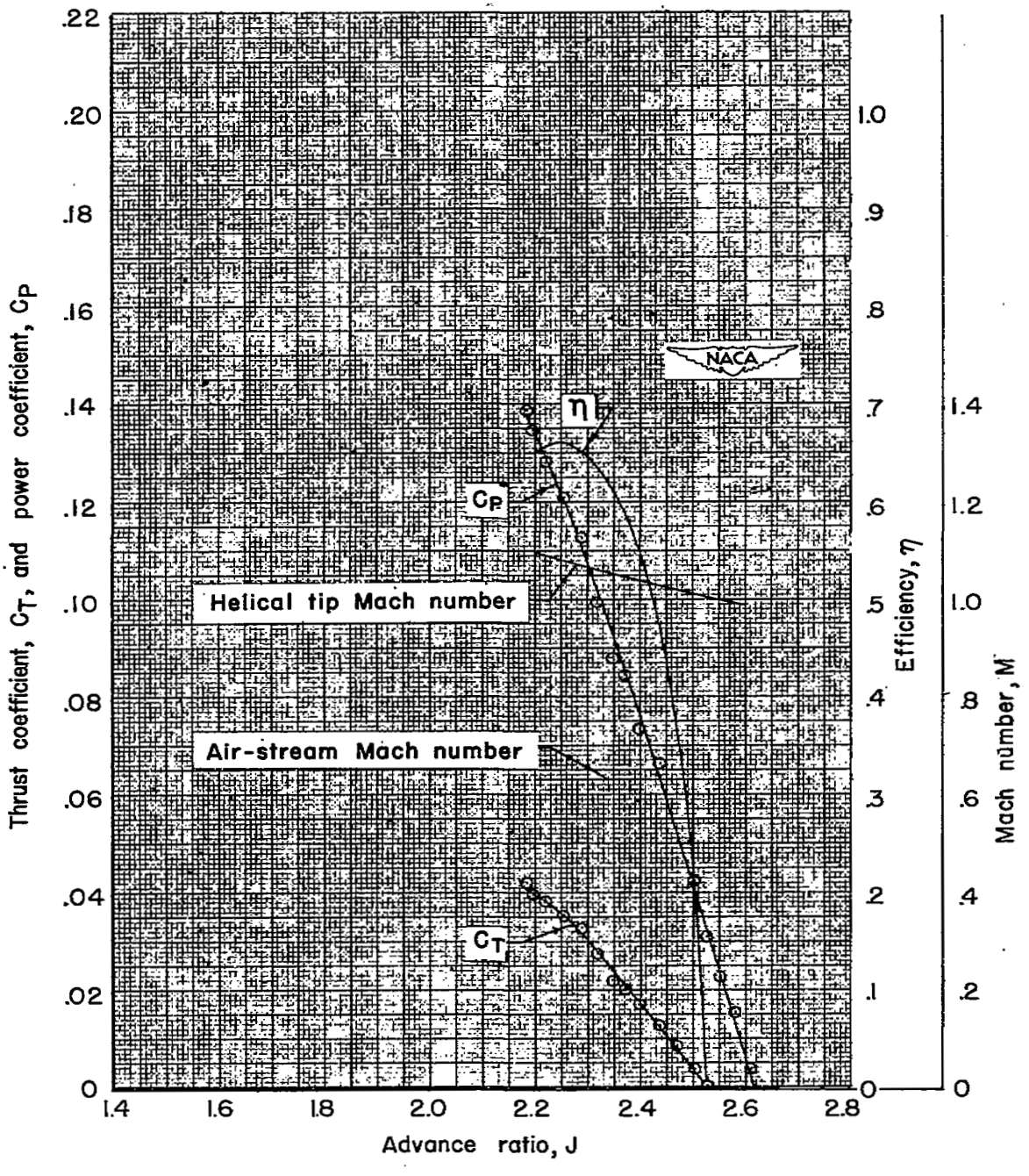

(d) Air-stream Mach number at maximum efficiency, 0.630.

Figure 19.- Concluded.

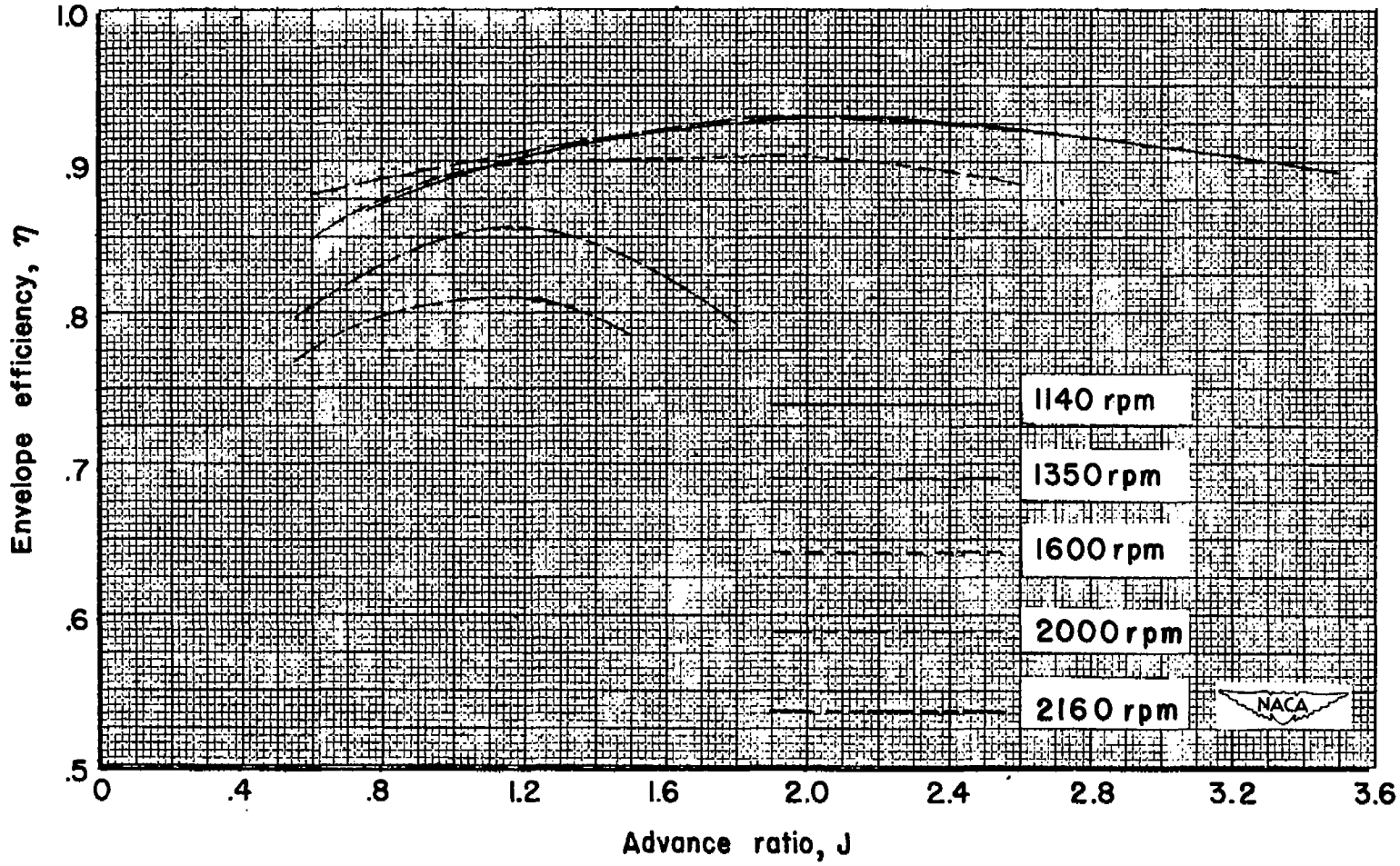

Figure 20.- Propeller efficiency envelope curves for NACA 10-(4)(08)-03CY propeller.

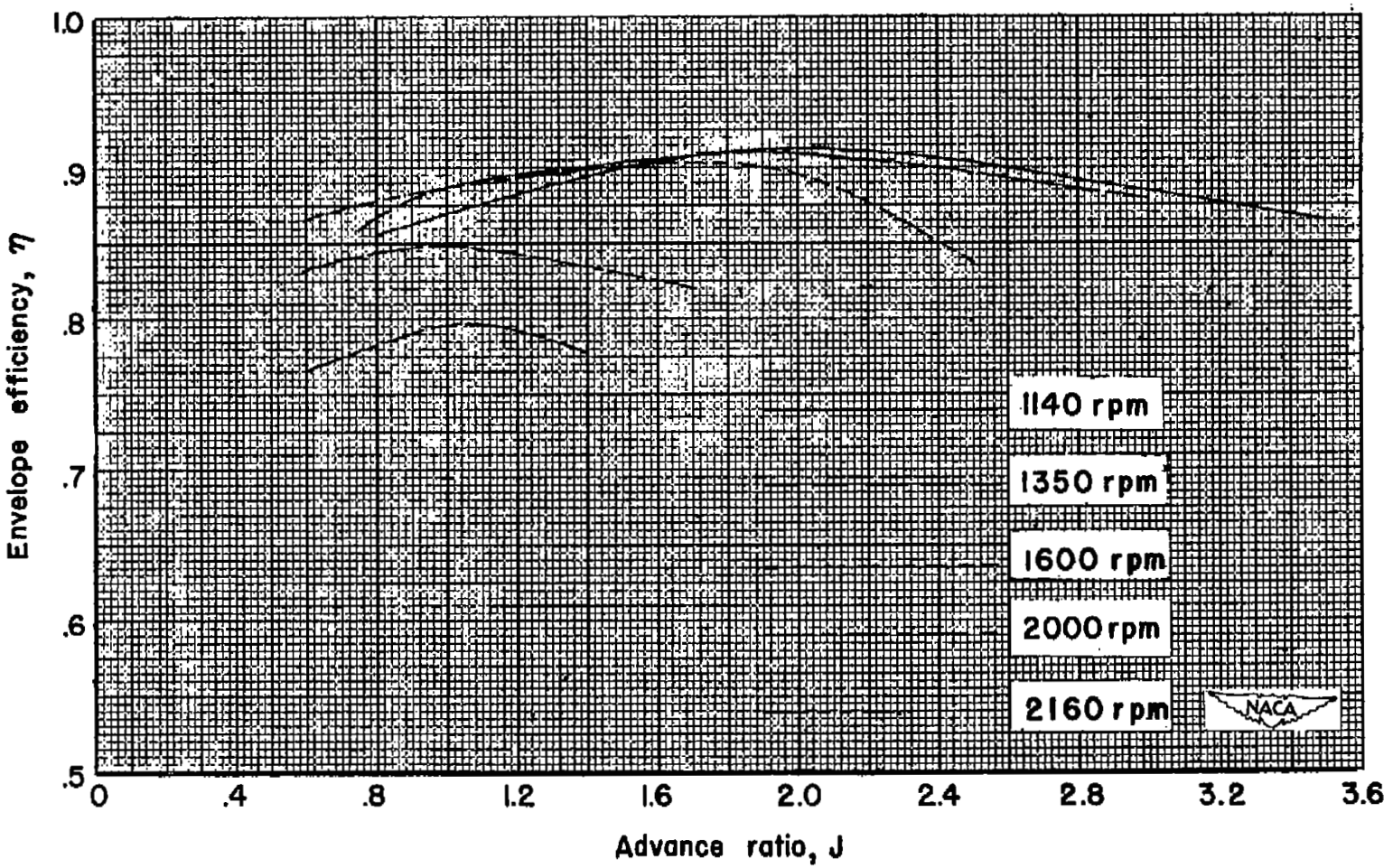

Figure 21.- Propeller efficiency envelope curves for NACA 10-(4)(08)-03RCY propeller.

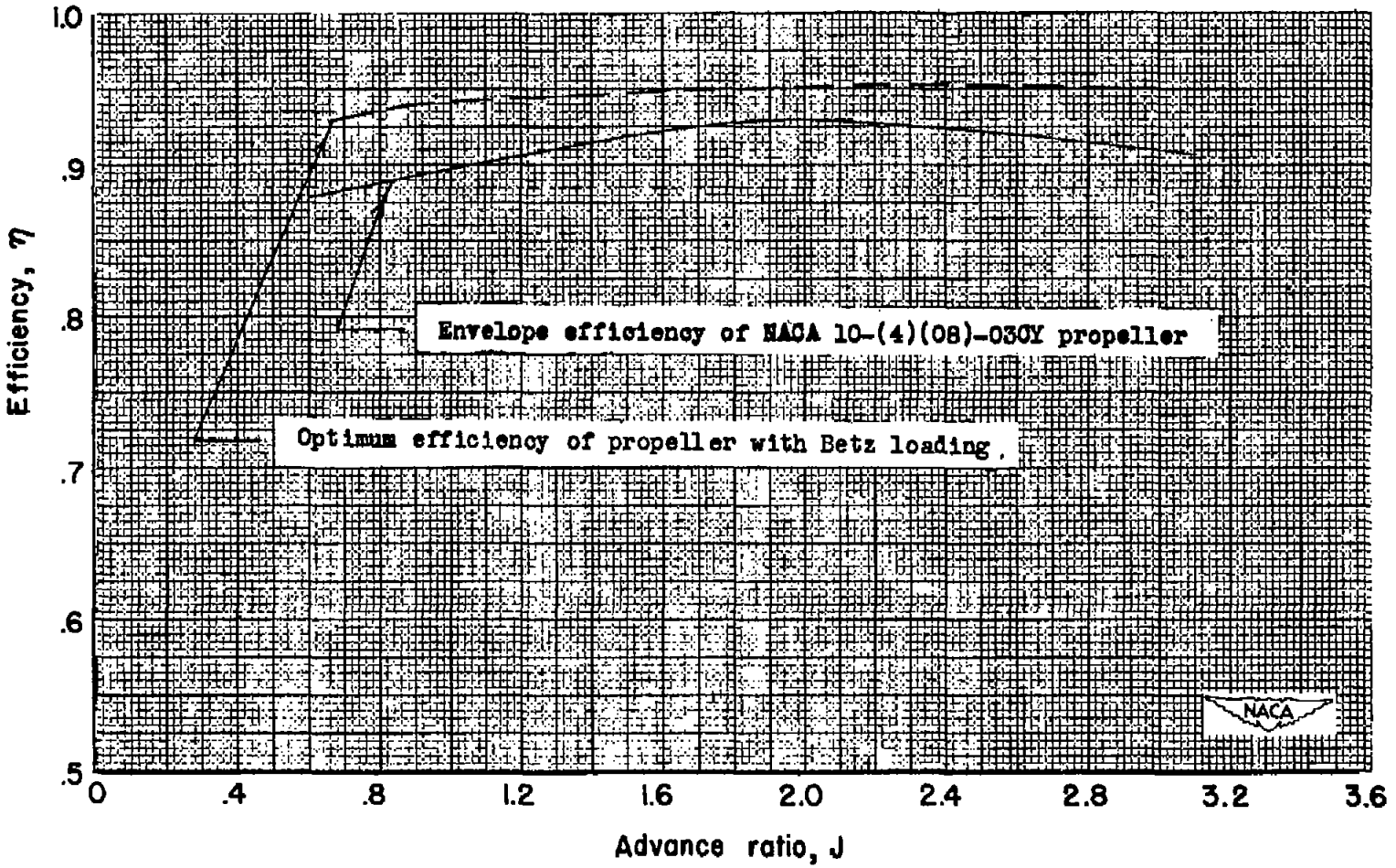

Figure 22.- Comparison of envelope efficiency of NACA 10-(4)(08)-03CY propeller at 1350 rpm with optimum efficiency of the two-blade propeller with Betz loading.

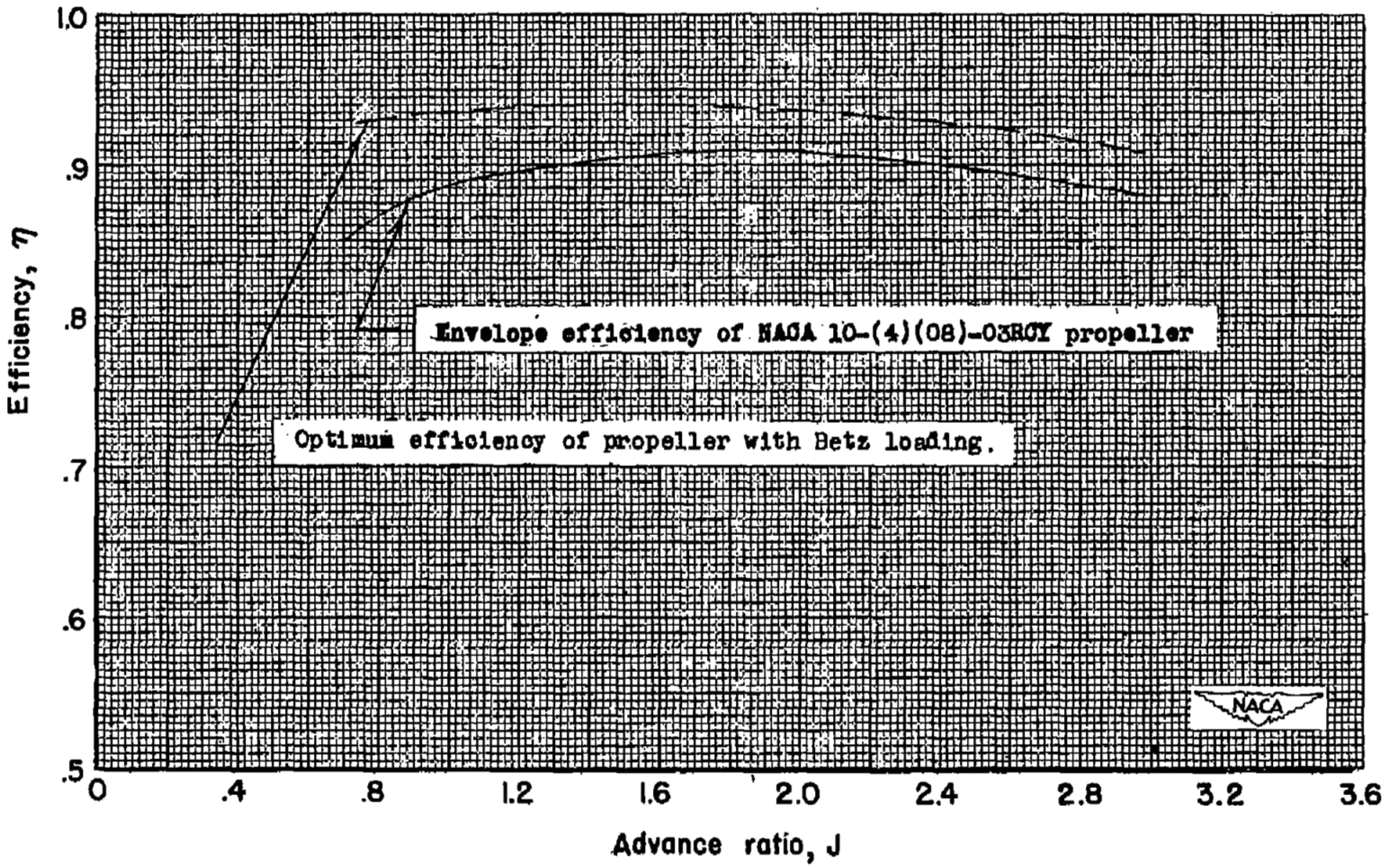

Figure 23.- Comparison of envelope efficiency of NACA 10-(4)(08)-03RCY propeller at 1350 rpm with optimum efficiency of the two-blade propeller with Betz loading.

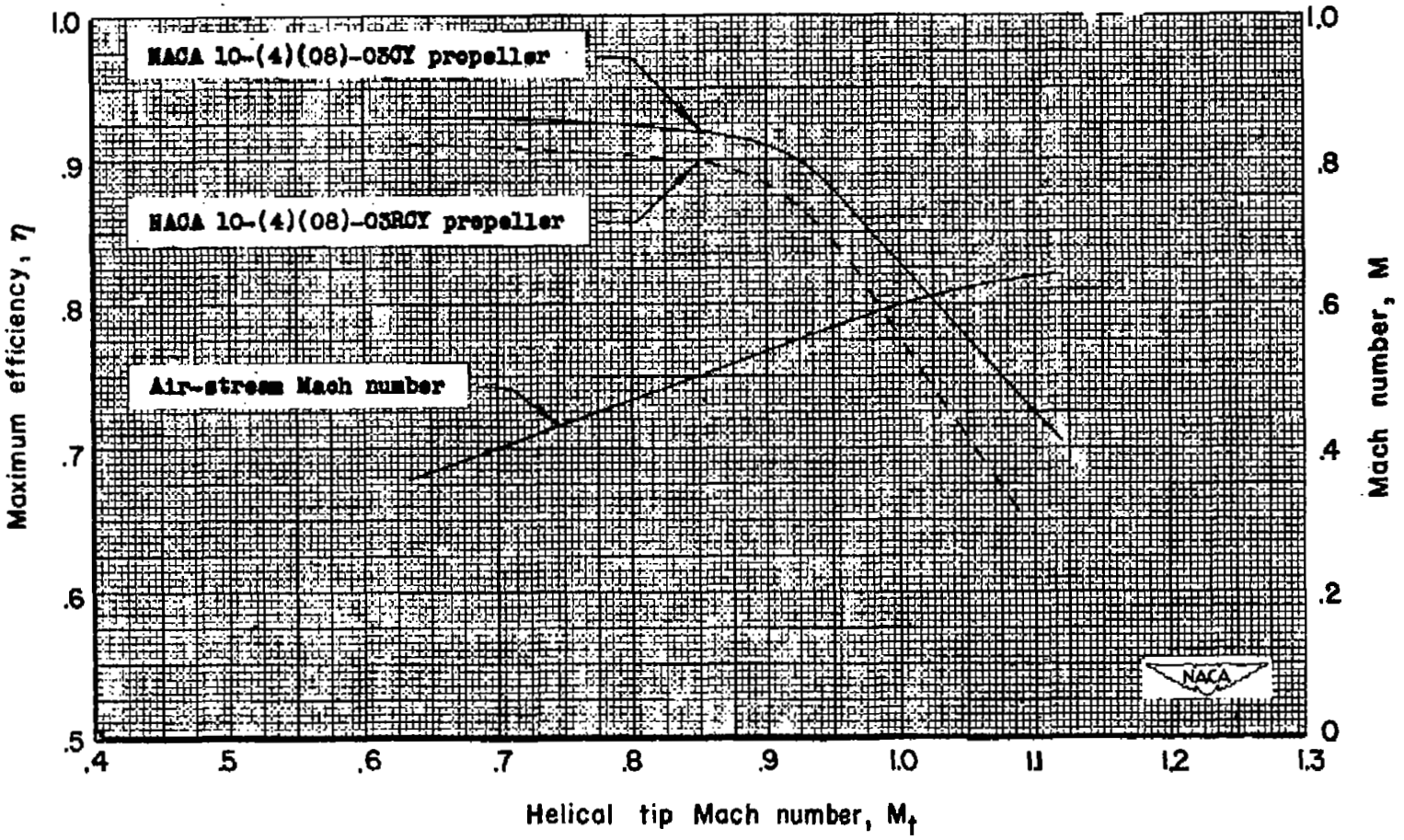

Figure 24.- Effect of compressibility on maximum efficiency of NACA 10-(4)(08)-03CY and 10-(4)(08)-03RCY propellers. $\beta_{0.75R} = 45^{\circ}$.

NASA Technical Library
3 1176 01436 6547